Computational light scattering (PAP315)

Lecture 14

Karri Muinonen[1,2]
Professor of Astronomy
[1]Department of Physics, University of Helsinki, Finland
[2]Finnish Geospatial Research Institute (FGI), Masala, Finland

Contents

Introduction

- Asteroids
  - are a key to Solar System evolution
  - cause an impact hazard for the humankind
  - offer valuable space resources
- Lightcurve inversion using Lommel-Seeliger ellipsoids and convex shapes
  - rotation period, pole orientation, shape
  - phase curve parameters, light scattering
  - Gaia DR2 (Gaia Collaboration 2018)
- Phase curves vs. taxonomy
  - Oszkiewicz et al., JQSRT 2011
  - Muinonen et al., ESLAB53 Proc. 2019

- Markov-chain Monte Carlo methods (MCMC)
  - large numbers of parameters
- Example asteroids
  - (2867) Steins, (21) Lutetia, (26) Proserpina
  - ground-based data from DAMIT (Durech et al. 2010)
- Plane of scattering, solar phase angle
- References to lightcurve inversion
  - Russell, ApJ 1906, Kaasalainen et al. A&A 1992ab, Icarus 2001, Kaasalainen & Torppa, Icarus 2001, Torppa et al. 2003, Lamberg, Ph.D. thesis 1993, Durech et al., 2015
  - Cellino et al. A&A 2009, PSS 2015, Wang et al. 2015 & 2019, Muinonen & Lumme 2015, Muinonen et al. PSS 2015, Torppa et al. 2018
- Radio occultations
  - Lehtinen et al. 2018, Harju et al. 2018

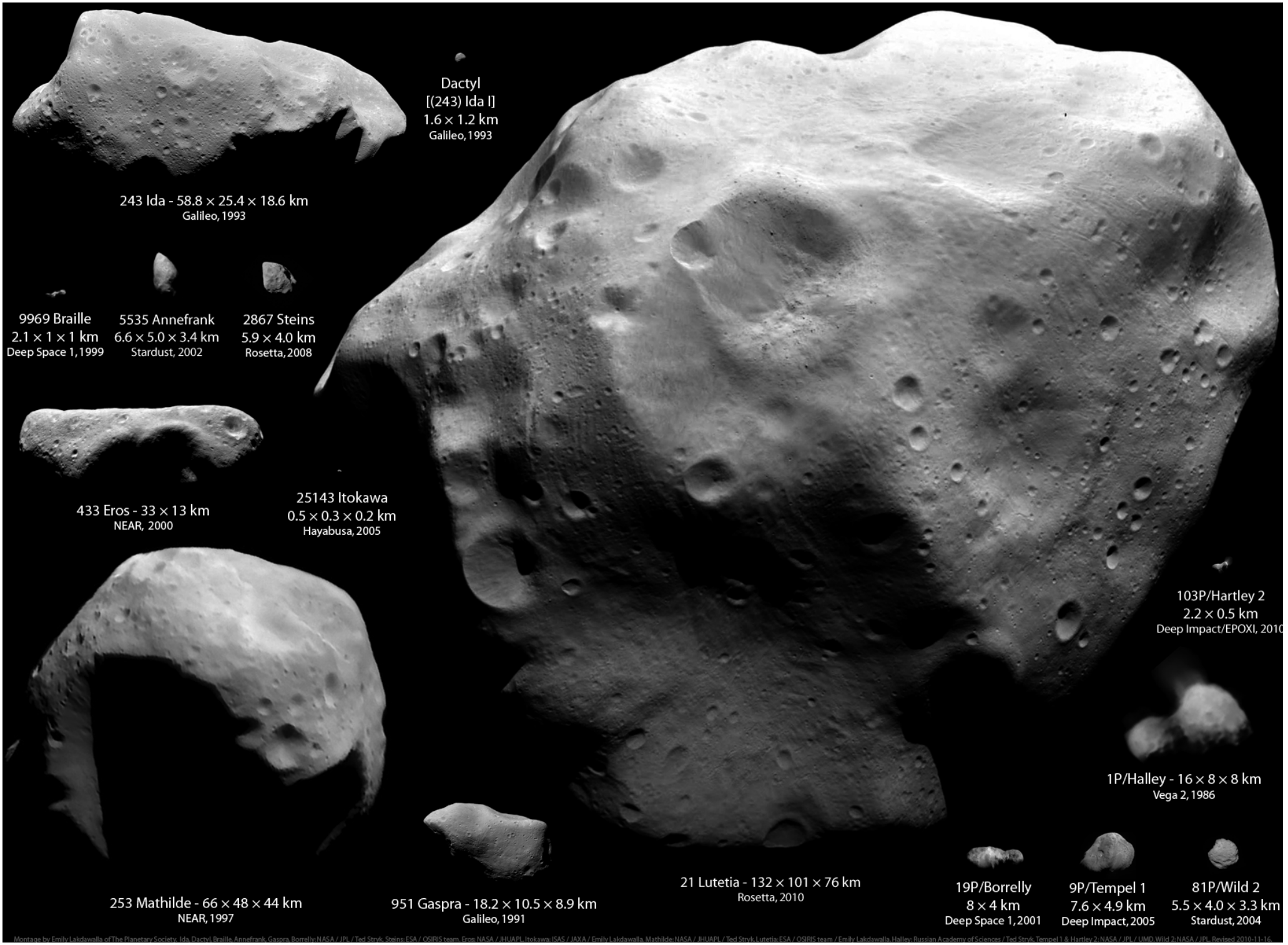
Dactyl
[(243) Ida I]
1.6 × 1.2 km
Galileo, 1993
243 Ida - 58.8 × 25.4 × 18.6 km
Galileo, 1993
9969 Braille
2.1 × 1 × 1 km
Deep Space 1, 1999
5535 Annefrank
6.6 × 5.0 × 3.4 km
Stardust, 2002
2867 Steins
5.9 × 4.0 km
Rosetta, 2008
433 Eros - 33 × 13 km
NEAR, 2000
25143 Itokawa
0.5 × 0.3 × 0.2 km
Hayabusa, 2005
103P/Hartley 2
2.2 × 0.5 km
Deep Impact/EPOXI, 2010
1P/Halley - 16 × 8 × 8 km
Vega 2, 1986
253 Mathilde - 66 × 48 × 44 km
NEAR, 1997
951 Gaspra - 18.2 × 10.5 × 8.9 km
Galileo, 1991
21 Lutetia - 132 × 101 × 76 km
Rosetta, 2010
19P/Borrelly
8 × 4 km
Deep Space 1, 2001
9P/Tempel 1
7.6 × 4.9 km
Deep Impact, 2005
81P/Wild 2
5.5 × 4.0 × 3.3 km
Stardust, 2004
Montage by Emily Lakdawalla of The Planetary Society. Ida, Dactyl, Braille, Annefrank, Gaspra, Borrelly: NASA / JPL / Ted Stryk. Steins: ESA / OSIRIS team. Eros: NASA / JHUAPL. Itokawa: ISAS / JAXA / Emily Lakdawalla. Mathilde: NASA / JHUAPL / Ted Stryk. Lutetia: ESA / OSIRIS team / Emily Lakdawalla. Halley: Russian Academy of Sciences / Ted Stryk. Tempel 1 & Hartley 2: NASA / JPL / UMD. Wild 2: NASA / JPL. Revised 2010-11-16.

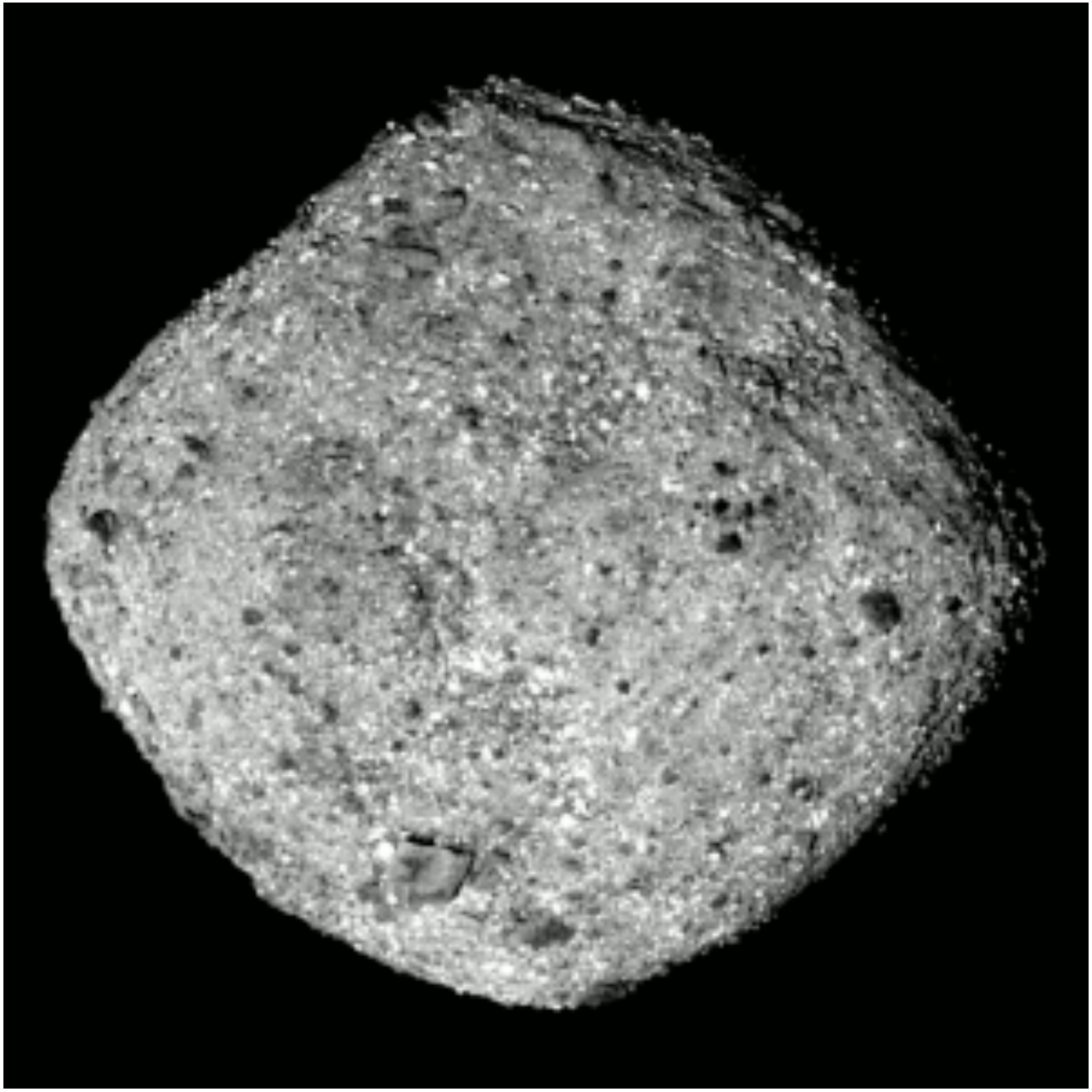

NASA OSIRIS-REx at (101955) Bennu

(21) Lutetia, early model and example dense Ground-based lightcurves, Torppa et al., Icarus 2003, obs. ref. therein

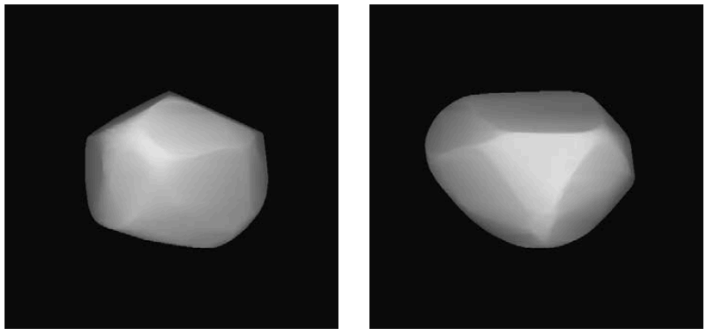

Fig. 17. Shape model of 21 Lutetia.

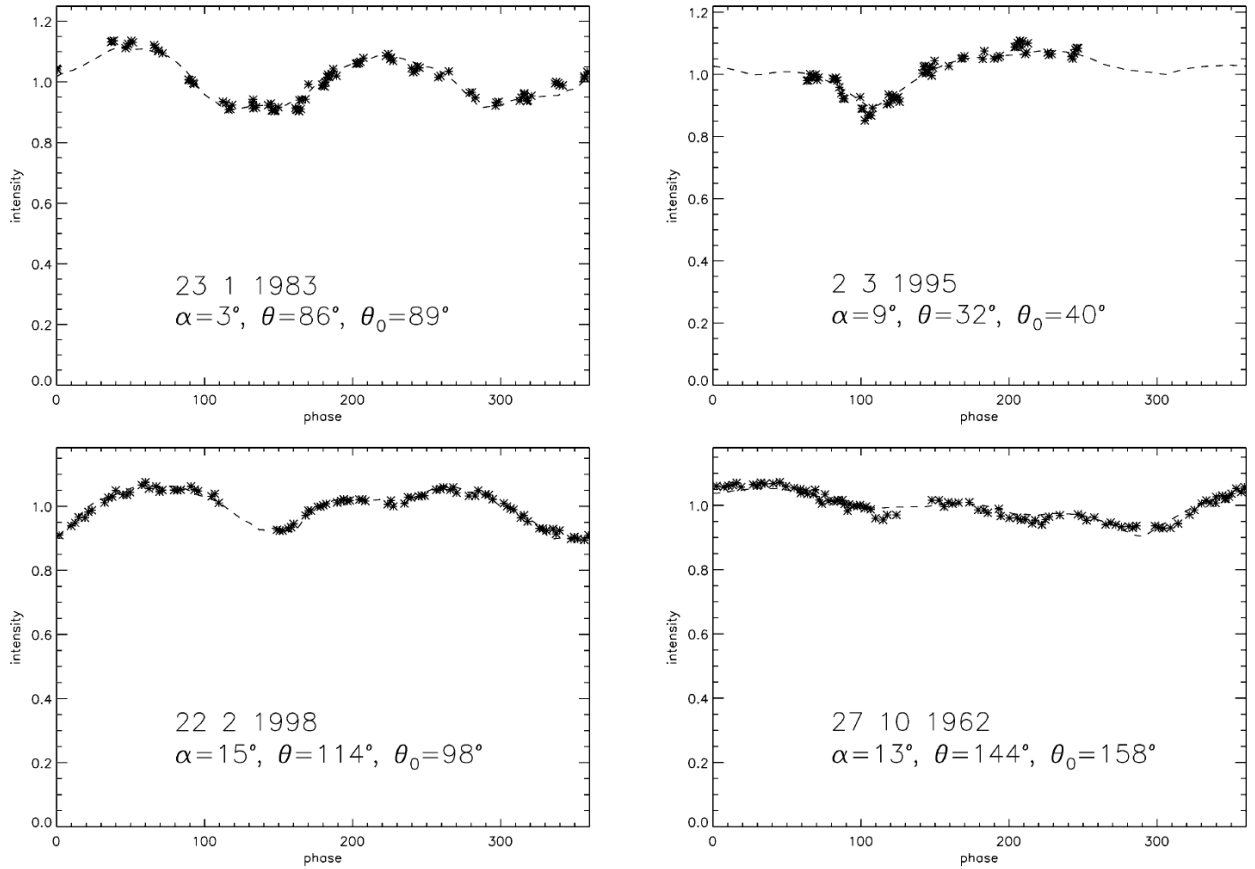

Fig. 18. Four lightcurves of 21 Lutetia with model fits.

Asteroid (171) Ophelia

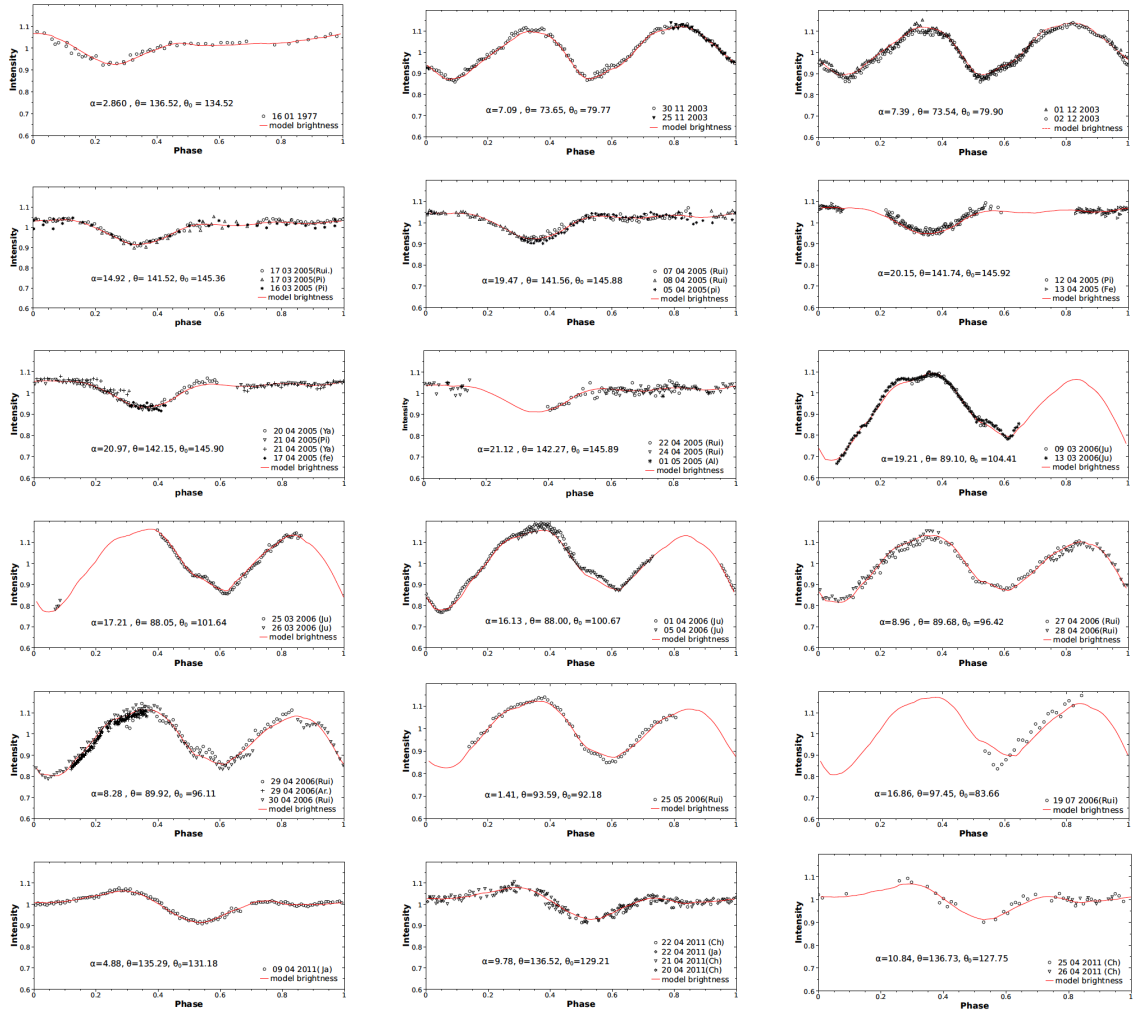

Fig. 3. The lightcurves for (171) Ophelia folded with the period of 6.665429 h.

Wang et al. 2015, A&A

Asteroid (171) Ophelia

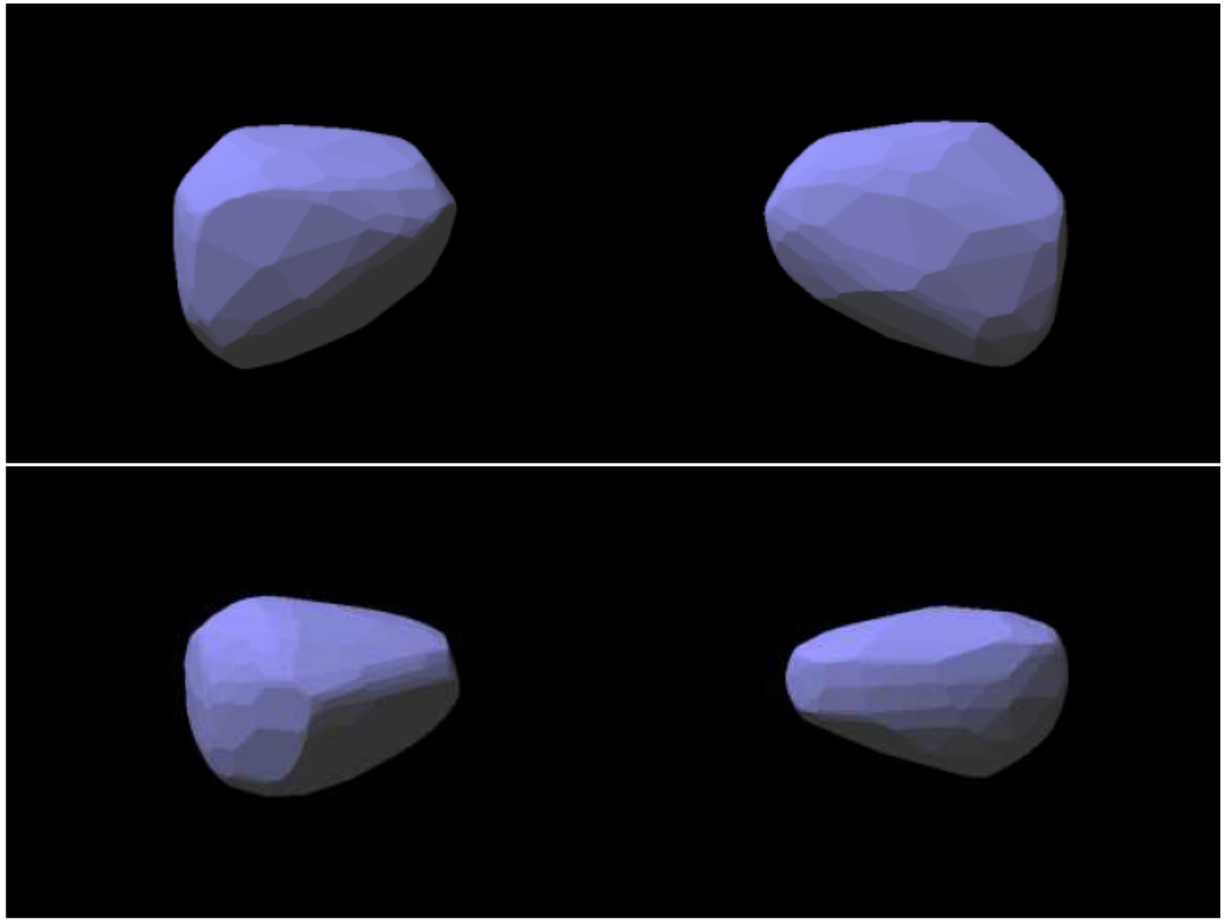

Fig. 2. The convex shape of (171) Ophelia. The upper plots correspond to the pole-on view and the bottom plots to the equatorial view. Shapes are depicted for two pole solutions: (152°, 36°) (left) and (317°, 28°) (right).

Asteroid (171) Ophelia

Table 2. The relative triaxial dimensions for the convex shape models of (171) Ophelia. We give the axial ratios due to the definitions by Kaasalainen et al. (2002a; column 2) and by Torppa et al. (2008; column 3), as well as their average (column 4).

Pole, Period	Dimensions I	Dimensions II	Mean
(152°, +36°)	$a/b = 1.23$	$a/b = 1.23$	$a/b = 1.23$
6.665429 h	$b/c = 1.20$	$b/c = 1.19$	$b/c = 1.20$
(317°, +28°)	$a/b = 1.20$	$a/b = 1.23$	$a/b = 1.22$
6.665429 h	$b/c = 1.27$	$b/c = 1.26$	$b/c = 1.27$

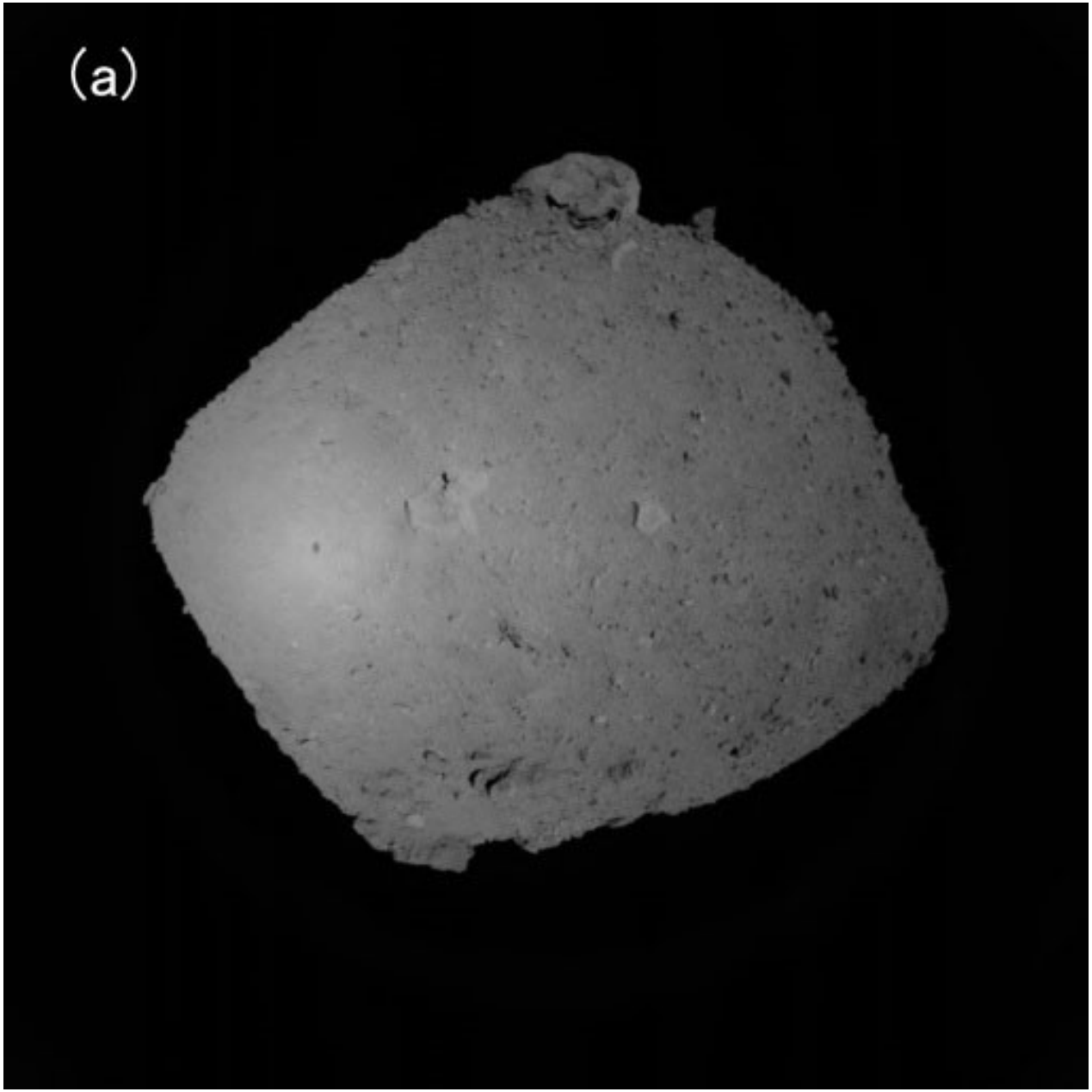

JAXA Hayabusa2 at (162173) Ryugu

Photometric and polarimetric phase curves for asteroids, Muinonen et al., CUP 2019, obs. ref. therein

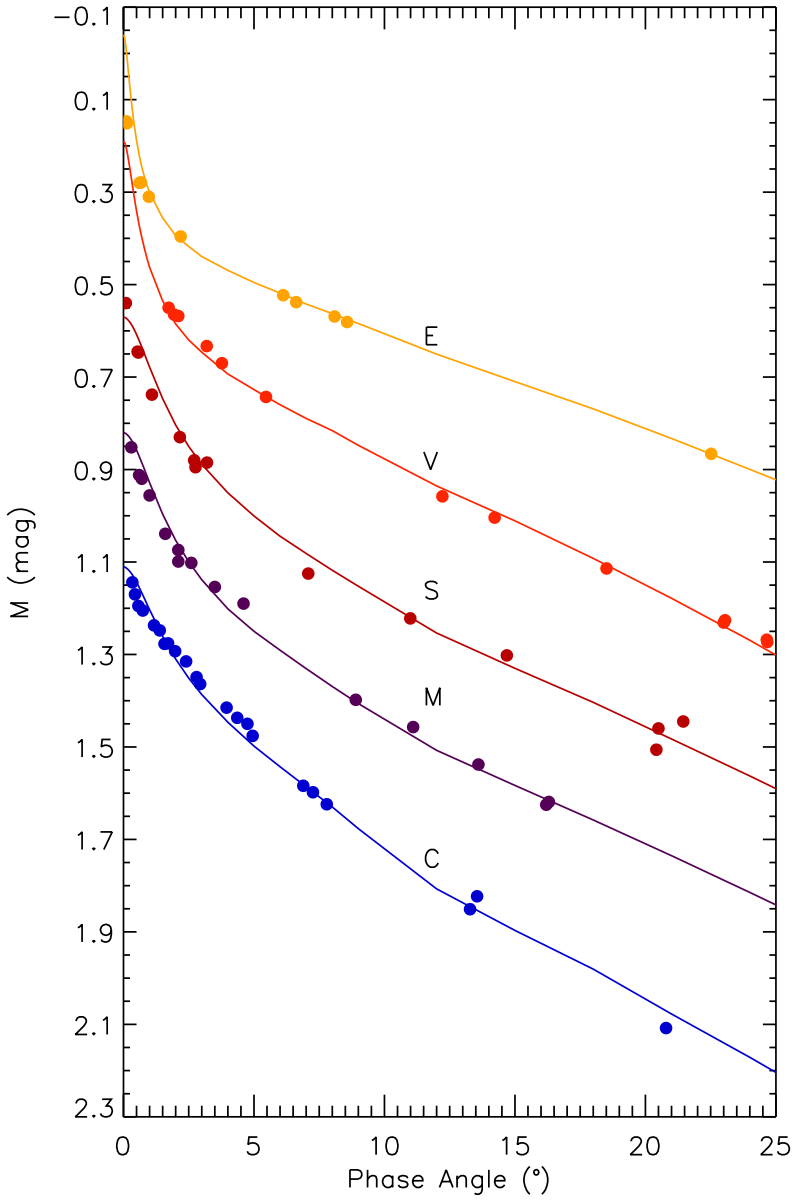

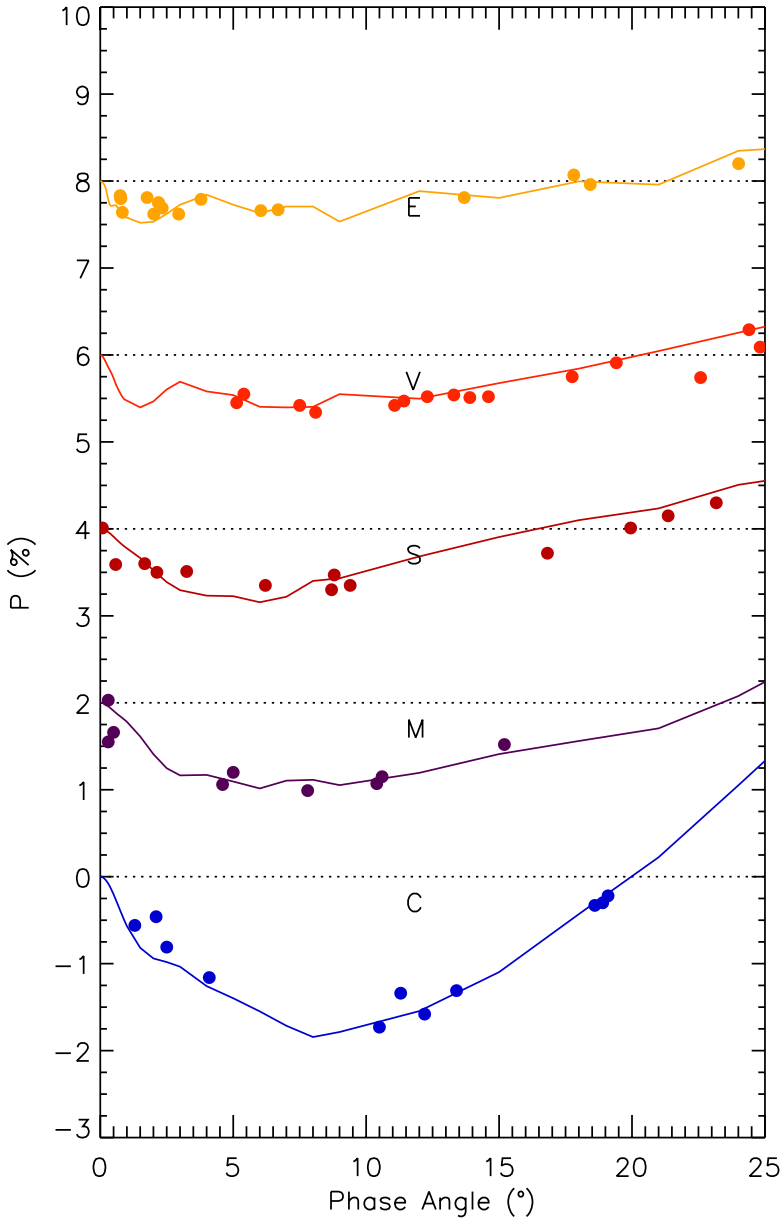

European Research Council

ERC AdG SAEMPL 2013-2018

Markkanen et al., ApJL 2018

Muinonen et al., OL 2018

Asteroid forward modeling

Lommel-Seeliger reflection coefficient

$$R_{\rm LS}(\mu,\mu_0,\phi) = \frac{1}{4}\tilde{\omega}P(\alpha)\frac{1}{\mu+\mu_0}$$

Geometric albedo and scattering phase function, including the proper phase curve $\Phi_{HG_1G_2}$,

$$\frac{1}{8}\tilde{\omega}P(\alpha) = p\frac{\Phi_{HG_1G_2}(\alpha)}{\Phi_{\rm LSS}(\alpha)}$$

$$L_{\rm LSS}(\alpha) = \frac{1}{32}\pi F_0 D^2 \tilde{\omega}P(\alpha)\Phi_{\rm LS}(\alpha),$$

$$\Phi_{\rm LSS}(\alpha) = 1 - \sin\frac{1}{2}\alpha\ \tan\frac{1}{2}\alpha\ \ln(\cot\frac{1}{4}\alpha)$$

Final reflection coefficient (Muinonen et al., PSS 2015)

$$R_{\rm LS}(\mu,\mu_0,\phi) = 2p\frac{\Phi_{HG_1G_2}(\alpha)}{\Phi_{\rm LSS}(\alpha)}\frac{1}{\mu+\mu_0}$$

Disk-integrated brightness for a Lommel-Seeliger ellipsoid

$$L(\alpha) = \frac{1}{8}\,\pi F_0 \tilde{\omega} P(\alpha)\, abc \left\{ \frac{(S_\odot + S_\oplus)(S_\odot S_\oplus + s_{\odot\oplus})}{S} - \frac{S_\odot^2 S_\oplus^2 - s_{\odot\oplus}^2}{S^3} \ln \left| \frac{S + S_\odot + S_\oplus}{S - S_\odot - S_\oplus} \right| \right\},$$

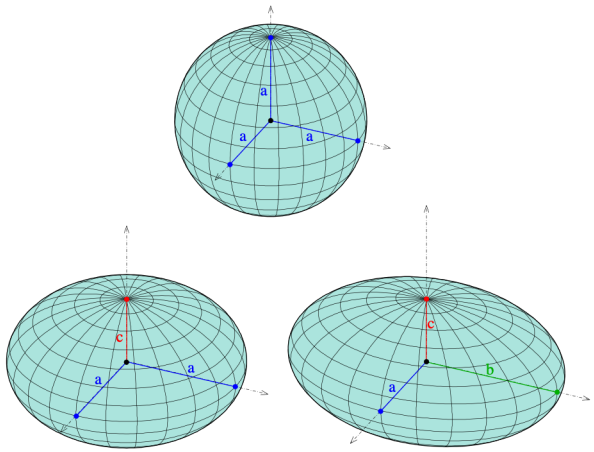

where

$$S = \sqrt{S_\odot^2 + S_\oplus^2 + 2 s_{\odot\oplus}},$$

$$S_\odot = \sqrt{\mathbf{e}_\odot^{\mathrm{T}} C \mathbf{e}_\odot},$$

$$S_\oplus = \sqrt{\mathbf{e}_\oplus^{\mathrm{T}} C \mathbf{e}_\oplus},$$

$$s_{\odot\oplus} = \mathbf{e}_\odot^{\mathrm{T}} C \mathbf{e}_\oplus.$$

$$C = \mathrm{diag}(a^{-2}, b^{-2}, c^{-2})$$

Parameters (unknowns):

$$(P, \lambda, \beta, \varphi_0, a, b, c, p, G_1, G_2, D)^T$$

Muinonen & Lumme, A&A 2015

Disk-integrated brightness for a convex model

Gaussian surface density:

$$G(\theta,\varphi) = \exp\left[\sum_{l_{\min}}^{l_{\max}}\sum_{m=-l}^{l} s_{lm}Y_{lm}(\theta,\varphi)\right]$$

Disk-integrated brightness:

$$L(\alpha) = \int_{A_+} dA\ \mu I(\mu,\mu_0,\alpha)$$

$$= \int_{A_+} dA\ \mu\mu_0 R(\mu,\mu_0,\alpha)F_0$$

Parameters (unknowns):

$$(P,\lambda,\beta,\varphi_0,s_{00},\ldots,s_{l_{\max}l_{\max}},p,G_1,G_2,D)^T$$

$$N_{\mathrm{P}} = 4+(l_{\max}+1)^2-l_{\min}^2+4$$

e.g., Muinonen et al., in prep. & Torppa et al., ASR 2018

Statistical inversion

- Observation equation:

$$\mathbf{M}_{\rm obs} = \mathbf{M}(\mathbf{P}) + \epsilon + \upsilon$$

$$\begin{aligned}\mathbf{M}_{\rm obs} &= (M_{{\rm obs},11},\ldots,M_{{\rm obs},1N_1};\ldots;\\ &\quad M_{{\rm obs},N_{\rm lc}1},\ldots,M_{{\rm obs},N_{\rm lc}N_{N_{\rm lc}}})^{\rm T},\\ \mathbf{M}(\mathbf{P}) &= (M_{11}(\mathbf{P}),\ldots,M_{1N_1}(\mathbf{P});\ldots;\\ &\quad M_{N_{\rm lc}1}(\mathbf{P}),\ldots,M_{N_{\rm lc}N_{N_{\rm lc}}}(\mathbf{P}))^{\rm T}\end{aligned}$$

- A posteriori probability density:

$$\begin{aligned}p_{\rm p}(\mathbf{P}) &\propto \exp\left[-\frac{1}{2}\chi^2(\mathbf{P})\right],\\ \chi^2(\mathbf{P}) &= \Delta\mathbf{M}^T(\mathbf{P})\Lambda^{-1}_{\epsilon+\upsilon}\Delta\mathbf{M}(\mathbf{P}).\end{aligned}$$

- Each lightcurve in its own block:

$$\begin{aligned}\chi^2(\mathbf{P}) &= \sum_{i=1}^{N_{\rm lc}}\Delta\mathbf{M}_i^T(\mathbf{P})\Lambda^{-1}_{\epsilon+\upsilon,i}\Delta\mathbf{M}_i(\mathbf{P}),\\ \Delta\mathbf{M}_i(\mathbf{P}) &= \mathbf{M}_{{\rm obs},i} - \mathbf{M}_i(\mathbf{P}),\end{aligned}$$

- Negligible systematic errors:

$$\Lambda_{\epsilon+\upsilon} \approx \Lambda_{\epsilon}$$

$$M_{\mathrm{obs},ij} - M_{ij}(\mathbf{P}) = 2.5 \lg \frac{L_{ij}(\mathbf{P})}{L_{\mathrm{obs},ij}} \approx -(2.5 \lg \mathrm{e}) \left[\frac{L_{\mathrm{obs},ij} - L_{ij}(\mathbf{P})}{L_{\mathrm{obs},ij}} \right]$$

$$\chi^2(\mathbf{P}) = \sum_{i=1}^{N_{\mathrm{lc}}} \frac{1}{\sigma_{\epsilon,i}^2} \sum_{j=1}^{N_i} \left[\frac{\ell_{\mathrm{obs},ij} - \ell_{ij}(\mathbf{P}) 10^{0.4 \Delta M_{i0}(\mathbf{P})}}{\ell_{\mathrm{obs},ij}} \right]^2$$

- Predominating systematic errors:

$$\Lambda_{\epsilon+\upsilon} \approx \Lambda_{\upsilon}$$

$$\chi^2(\mathbf{P}) \rightarrow \frac{1}{\sigma_{\upsilon}^2} \sum_{i=1}^{N_{\mathrm{lc}}} \frac{1}{N_i} \sum_{j=1}^{N_i} \left[m_{\mathrm{obs},ij} - m_{ij}(\mathbf{P}) \right]^2$$

Virtual-observation MCMC

- Add random error:

$$\mathbf{M}_{\mathrm{v}} = \mathbf{M}_{\mathrm{obs}} + \epsilon_{\mathrm{v}}$$

- Probability density for virtual least squares parameters:

$$p_{\mathrm{V}}(\mathbf{P}_{\mathrm{v}}) = \int d\mathbf{M}_{\mathrm{v}} \delta(\mathbf{P}_{\mathrm{v}} - \mathbf{P}_{\mathrm{v}}(\mathbf{M}_{\mathrm{v}})) p(\mathbf{M}_{\mathrm{v}})$$

- Proposal probability density for MCMC:

$$p_{\mathrm{t}}(\Delta\mathbf{P}) = \int\int d\mathbf{P}_{\mathrm{v}} d\mathbf{P}'_{\mathrm{v}}\, \delta\left(\Delta\mathbf{P} - (\mathbf{P}_{\mathrm{v}} - \mathbf{P}'_{\mathrm{v}})\right) p_{\mathrm{V}}(\mathbf{P}_{\mathrm{v}}) p_{\mathrm{V}}(\mathbf{P}'_{\mathrm{v}})$$

- Practical implementation with repeated least squares:

$$\Delta\mathbf{P}_{jk} = \mathbf{P}_{\mathrm{v},j} - \mathbf{P}_{\mathrm{v},k}, \qquad j,k = 1,2,3\ldots,N_{\mathrm{v}};\ j \neq k$$

- Generate virtual observations by adding random errors to each observation
- Compute a virtual least-squares solution
- Repeat to obtain another solution
- In the parameter phase space, compute the difference vector
- Propose new parameters by adding the difference to the current parameters
- References for lightcurve inversion:
  - Muinonen et al., PSS 2015, Torppa et al. ASR 2018
  - Muinonen et al., in preparation

Inversion with ellipsoids

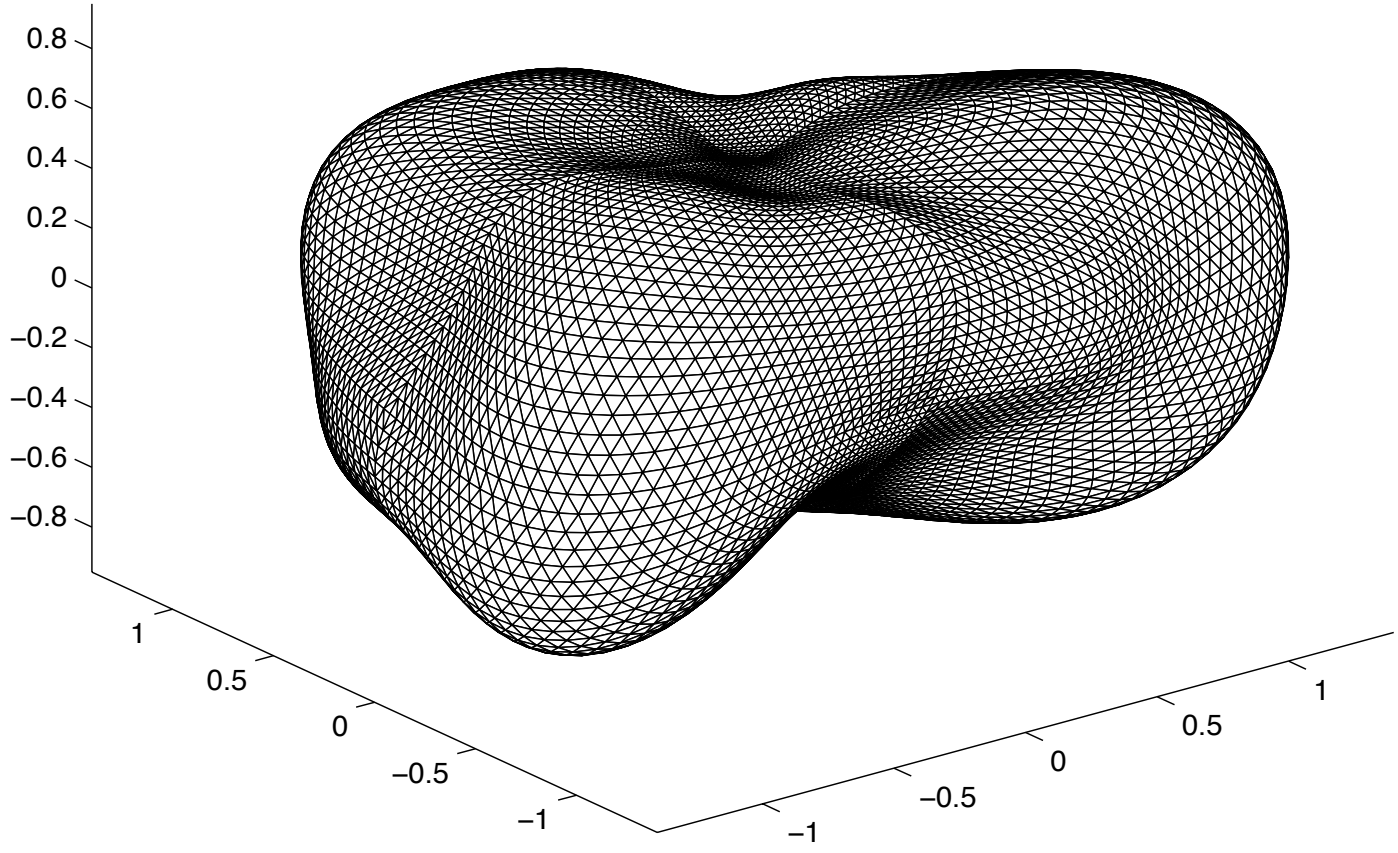

Gaussian-random-sphere asteroid (Muinonen et al. 2015, Wilkman et al. 2015)

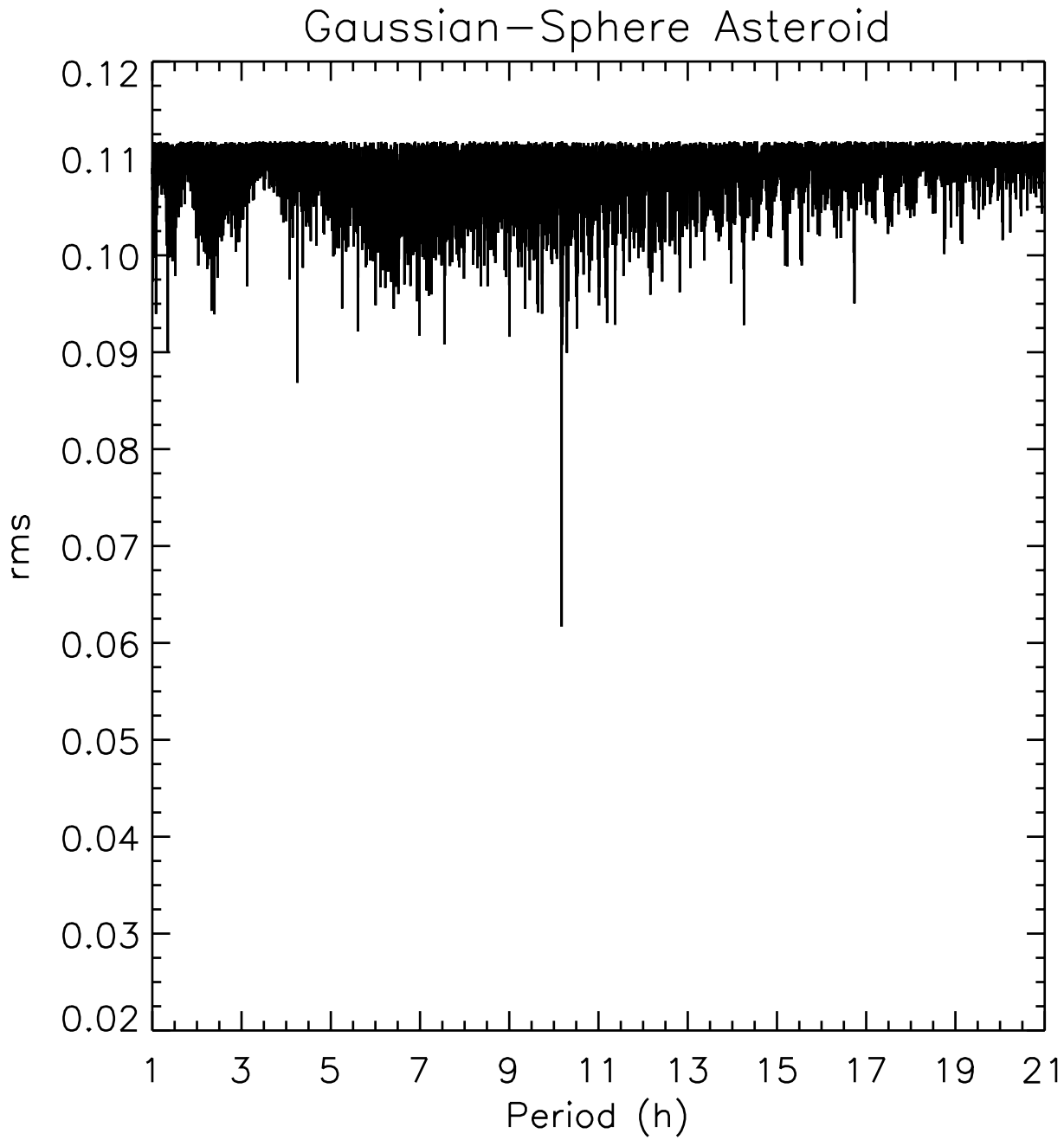
Gaussian−Sphere Asteroid
0.12
0.11
0.10
0.09
0.08
0.07
0.06
0.05
0.04
0.03
0.02
rms
1
3
5
7
9
11
13
15
17
19
21
Period (h)

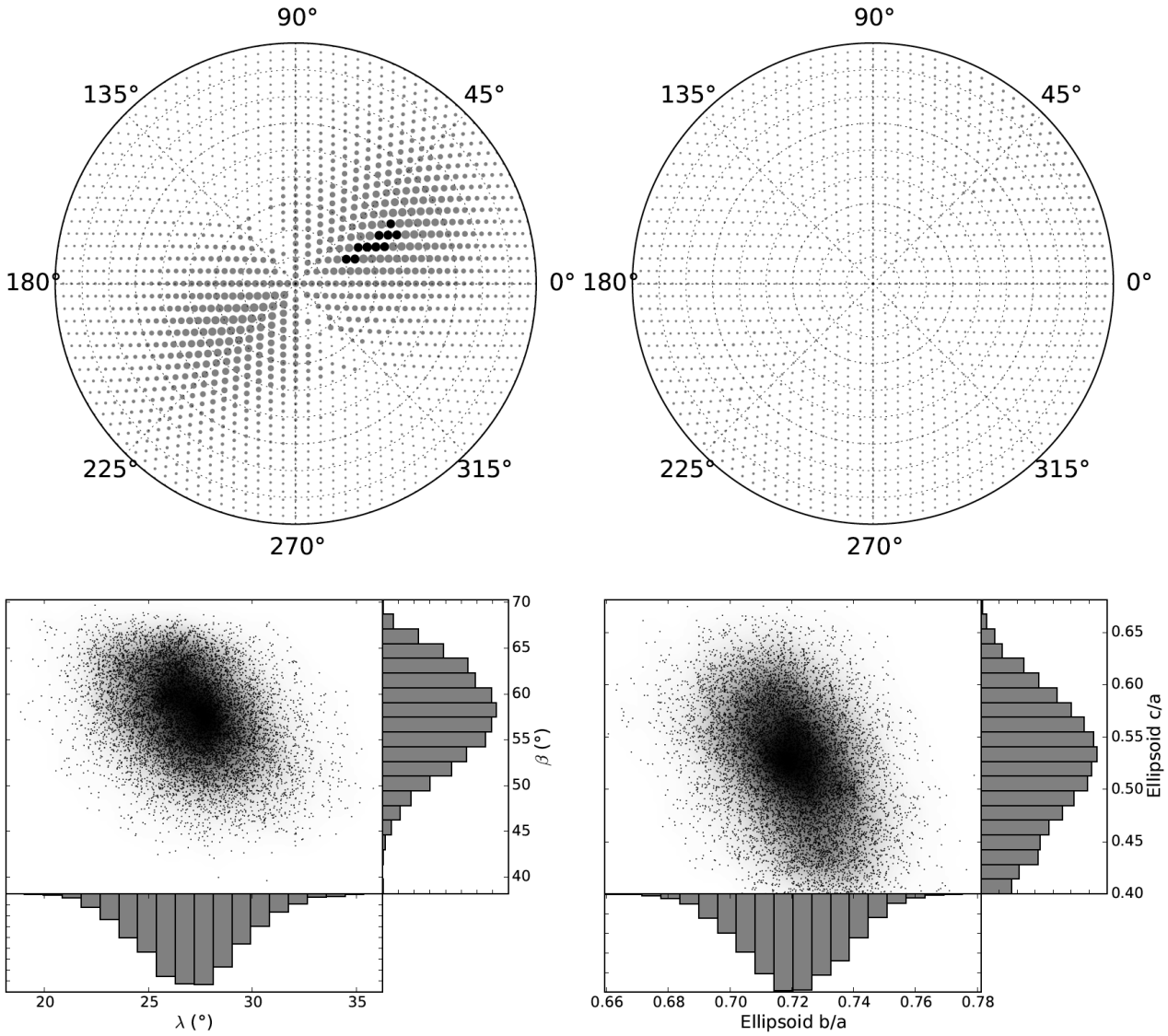

Figure 11: Ecliptic longitude and latitude of the pole scanned for the simulated Gaussian-sphere asteroid with a Lommel-Seeliger reflection coefficient by Torppa and Muinonen [38] with larger bullet size indicating better fits: maps for the northern (top left) and southern ecliptic hemispheres (top right). Black bullets indicate $\Delta\chi^2 < 10$ with respect to the best fit. Also shown are 10,000 MCMC sample poles (bottom left) and sample ellipsoid axial ratios (bottom right) with their one-dimensional marginal distributions.

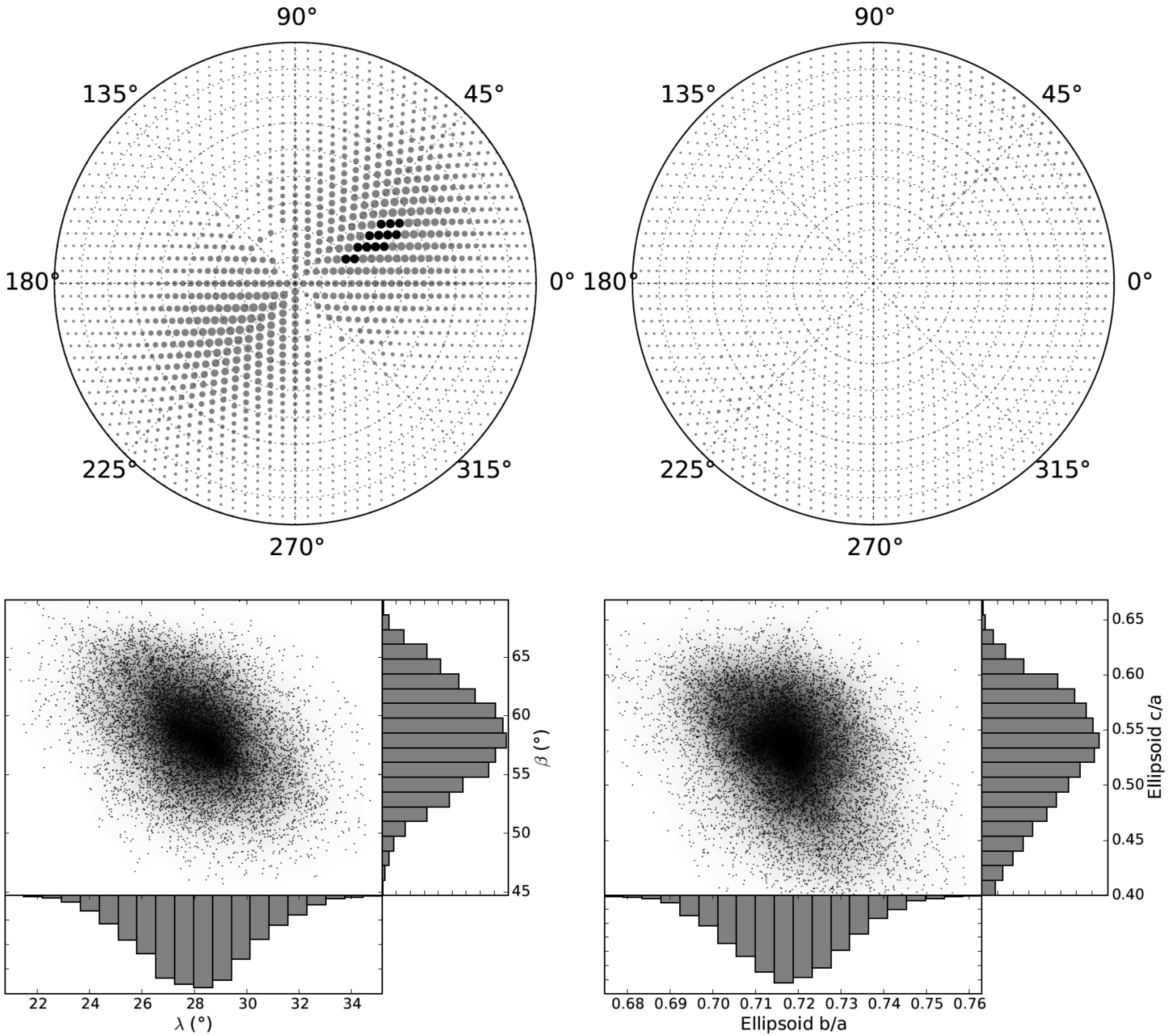

Figure 12: As in Fig. 11 for the Gaussian-sphere asteroid simulated with the numerical particulate-medium reflection coefficient.

Validation: (2867) Steins

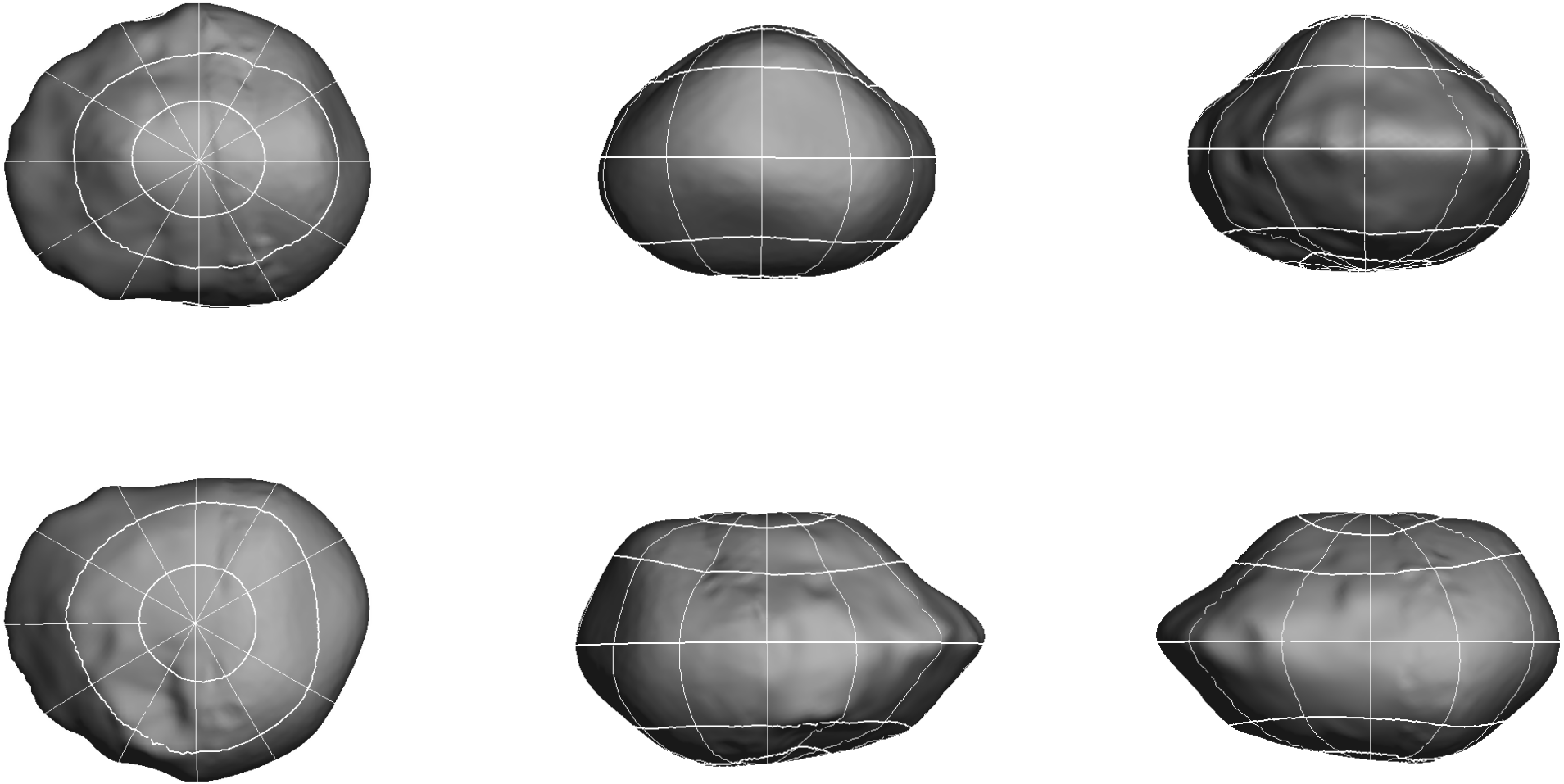

PDS

- Number of Gaia DR2 observations: 7
- Resolution in shape model (PDS): 5 deg
- Lommel-Seeliger scattering model
- H, G_1, G_2 phase function
  - Muinonen et al., Icarus 2010, Penttilä et al., PSS 2016
  - Shevchenko et al., PSS 2016
- E-class asteroids (spherical limit):
  - $G_1 = 0.1505$, $G_2 = 0.6005$
- Rotation period
  - P = 6.04681 h

- Pole orientation #1
  - λ = 94 deg, β = -85 deg
- Rotational phase at JD 51445.5:
  - ϕ = 244.2 deg
- Disk-integrated brightness, rms value:
  - σ = 0.026 mag
- Pole orientation #2
  - λ = 142 deg, β = -83 deg
- Rotational phase at JD 51445.5:
  - ϕ = 282.8 deg
- Disk-integrated brightness, rms value:
  - σ = 0.020 mag

Gaia DR2 data (7 observations)

Pole 1

Pole 2

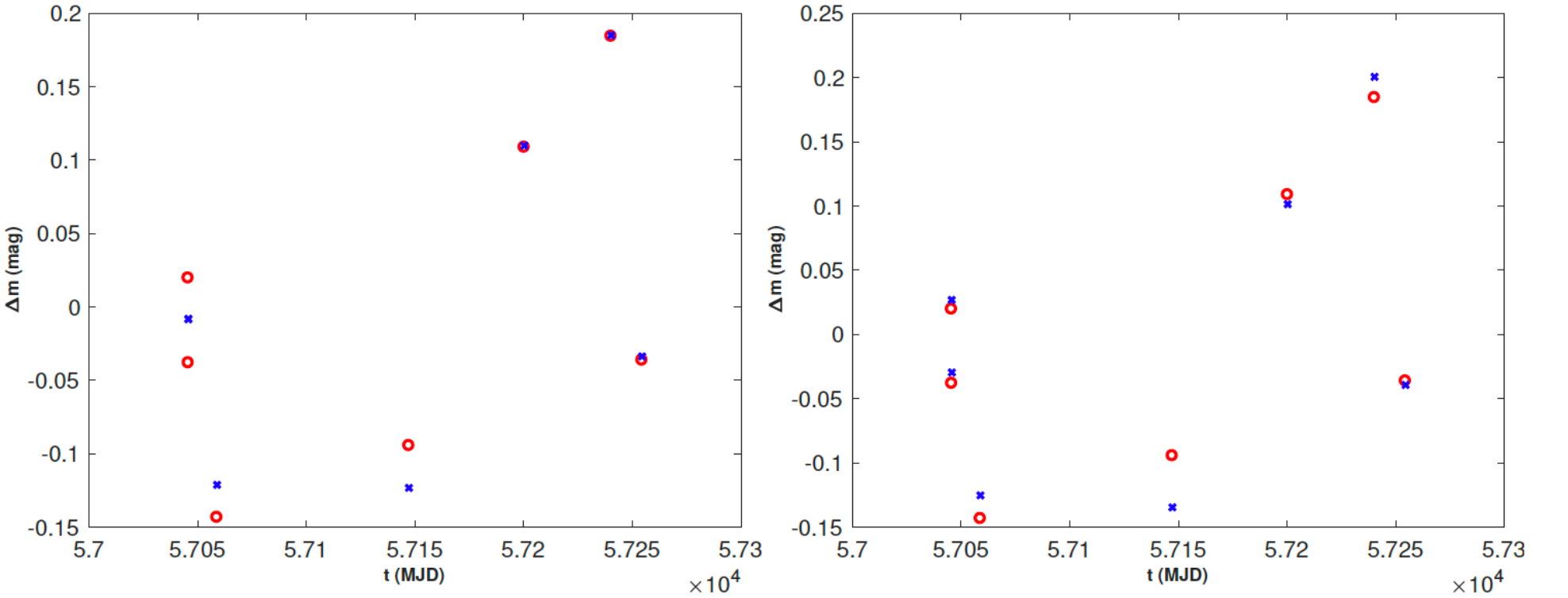

Red circles and blue crosses refer to the Gaia DR2 observations and the two pole models, respectively (Muinonen et al. 2019)

Convex inversion

Table 2. The asteroids incorporated in the present study. N and K denote the number of observations and lightcurves, respectively, and T_{obs} time span of the observations. For each asteroid, the uppermost numbers refer to the ground-based observations, the ones in the middle to the DR2 observations, and the lowermost numbers refer to the combined observations.

Asteroid	Class	N	K	T_{obs} (d)	T_{obs} (a)	References
(21) Lutetia	M	4012	50	17306.80	47.38	Gaia Collaboration (2018), Carry et al. (2010),
		8	1	435.65	1.19	Denchev et al. (1998), Lagerkvist et al. (1995),
		4020	51	19365.98	53.02	Dotto et al. (1992), Lupishko et al. (1987, 1983),
						Zappalá et al. (1984), Chang and Chang (1963)
(26) Proserpina	S	6664	29	1010.97	2.77	Gaia Collaboration (2018), Wang et al.
		43	1	542.78	1.49	
		6707	30	3038.92	8.32	
(585) Bilkis	C/D/P	1844	17	978.70	2.68	Gaia Collaboration (2018), Wang et al.
		33	1	621.66	1.70	
		1877	18	1563.78	4.28	
(2867) Steins	E	–	–	–		Gaia Collaboration (2018)
		7	1	208.86	0.57	
		7	1	208.86	0.57	

(21) Lutetia

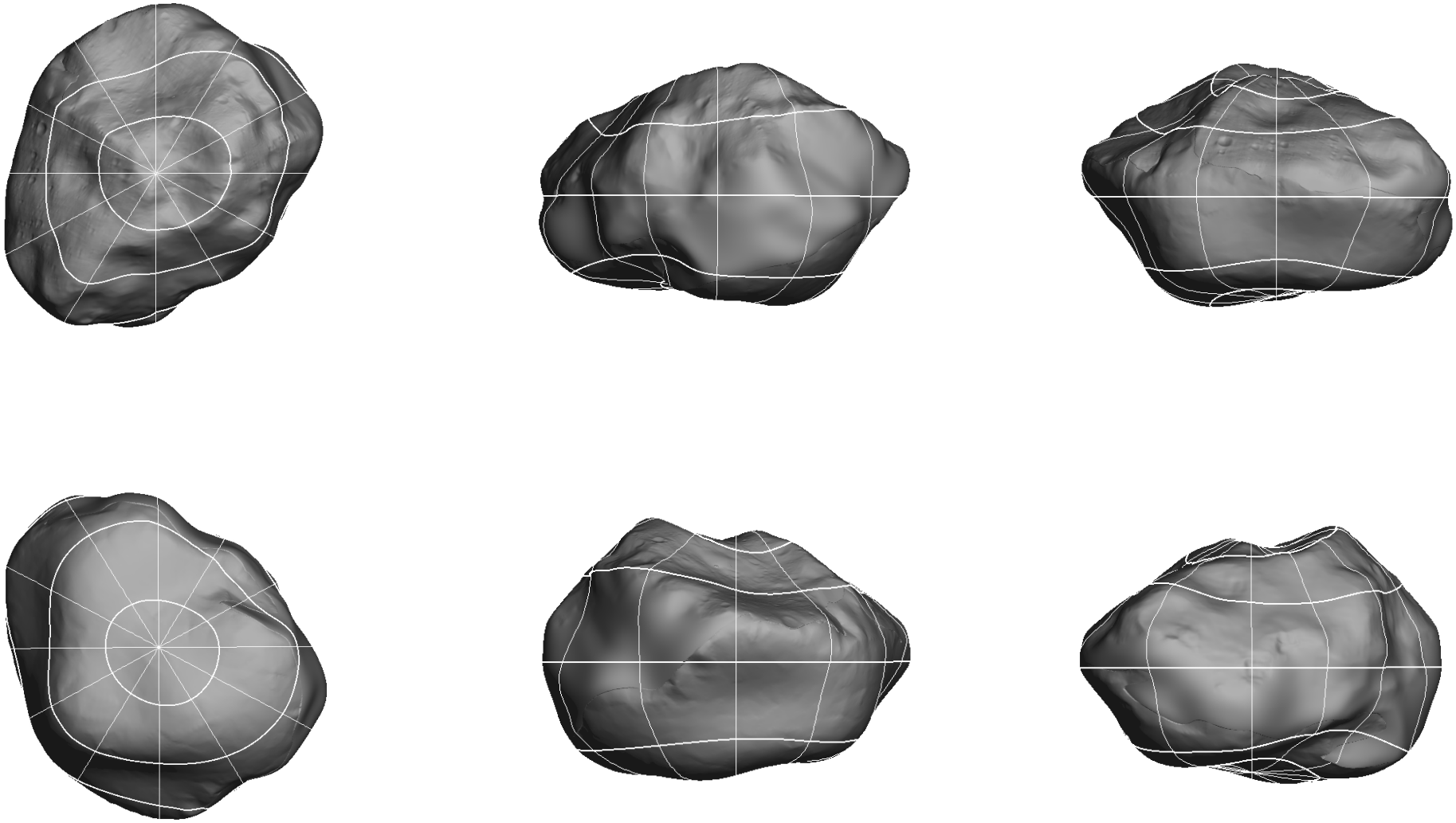

PDS

(21) Lutetia

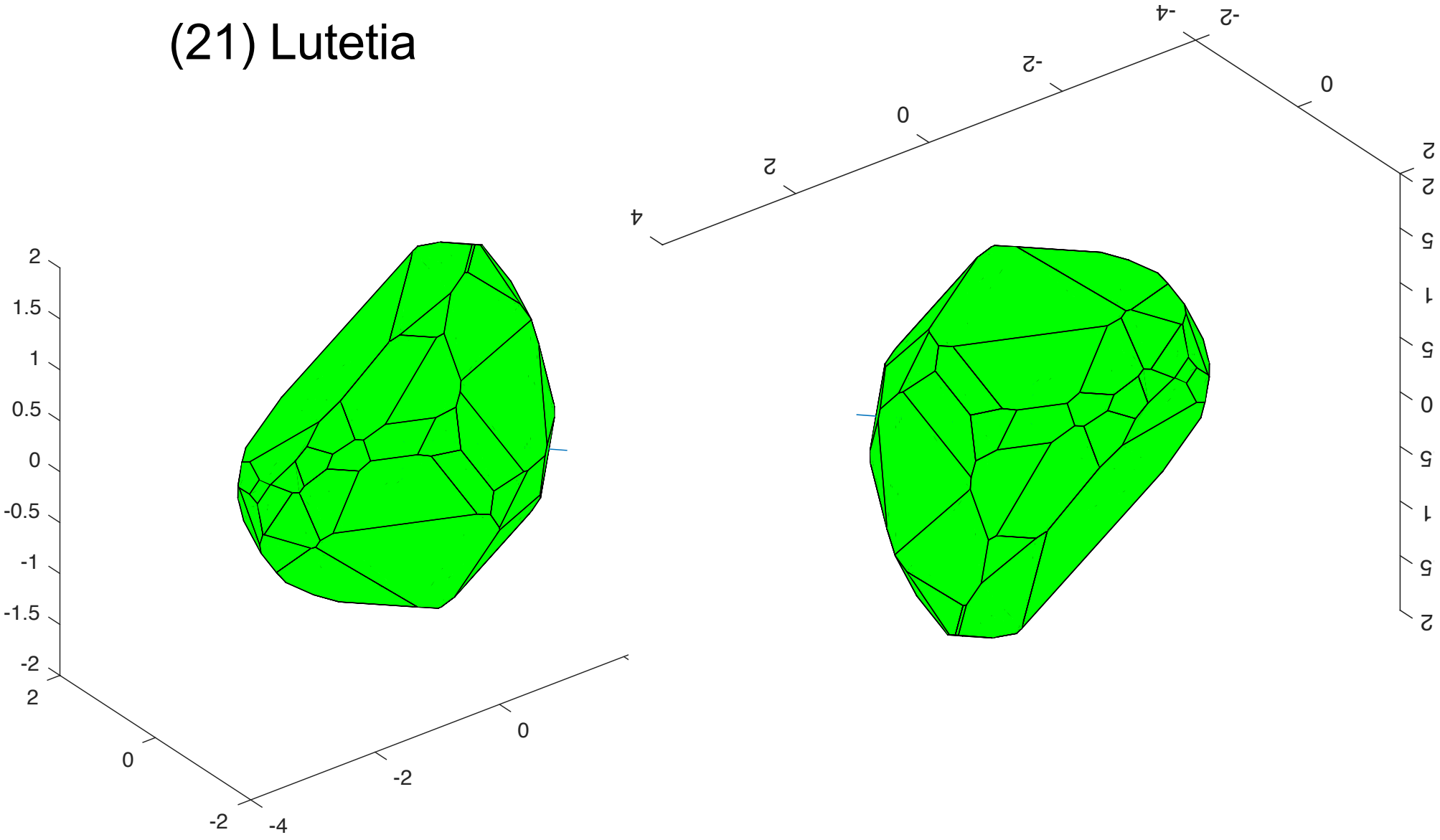

Convex inversion: (26) Proserpina

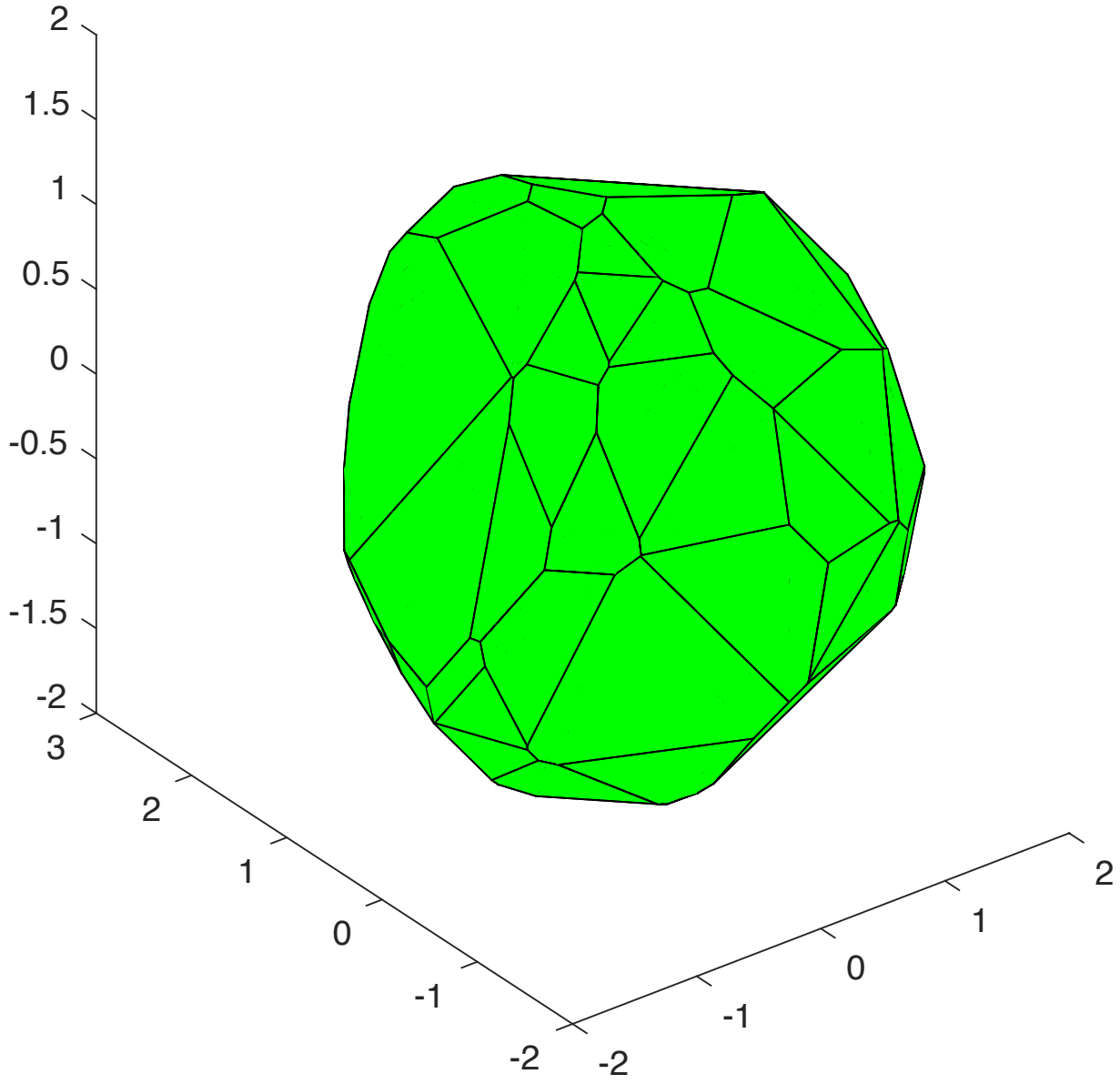

Gaia data only (43 obs., rms 0.016 mag, l_{max} = 4) convex MCMC inversion works!

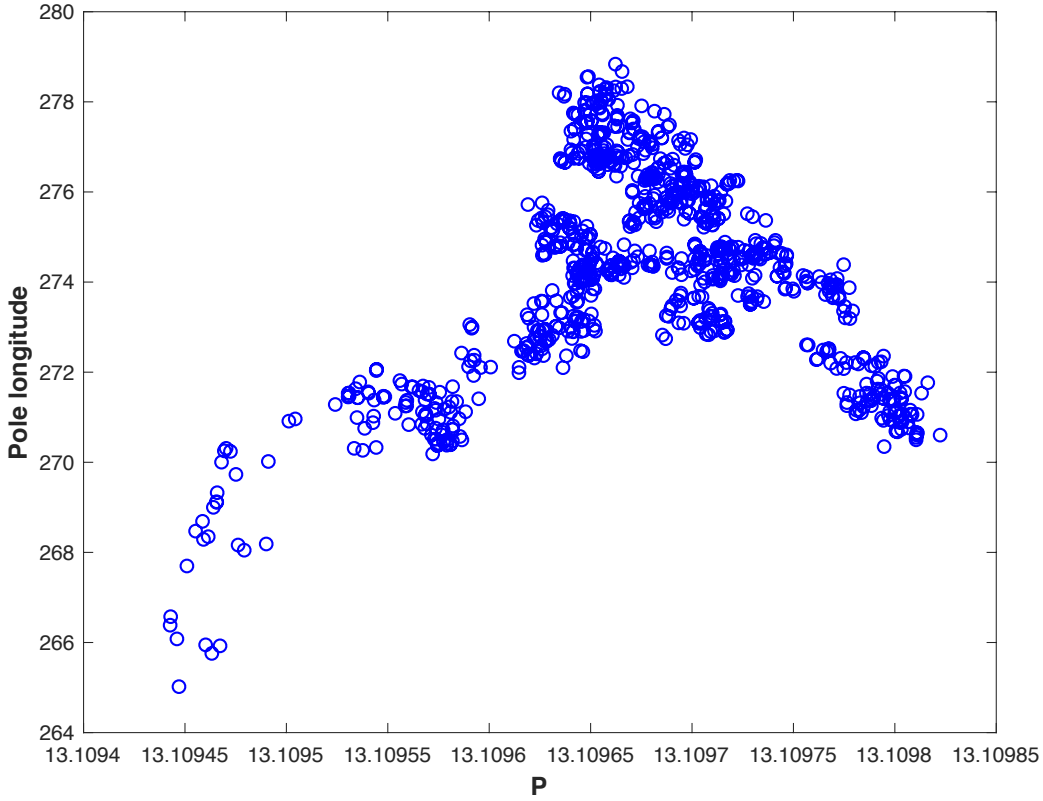

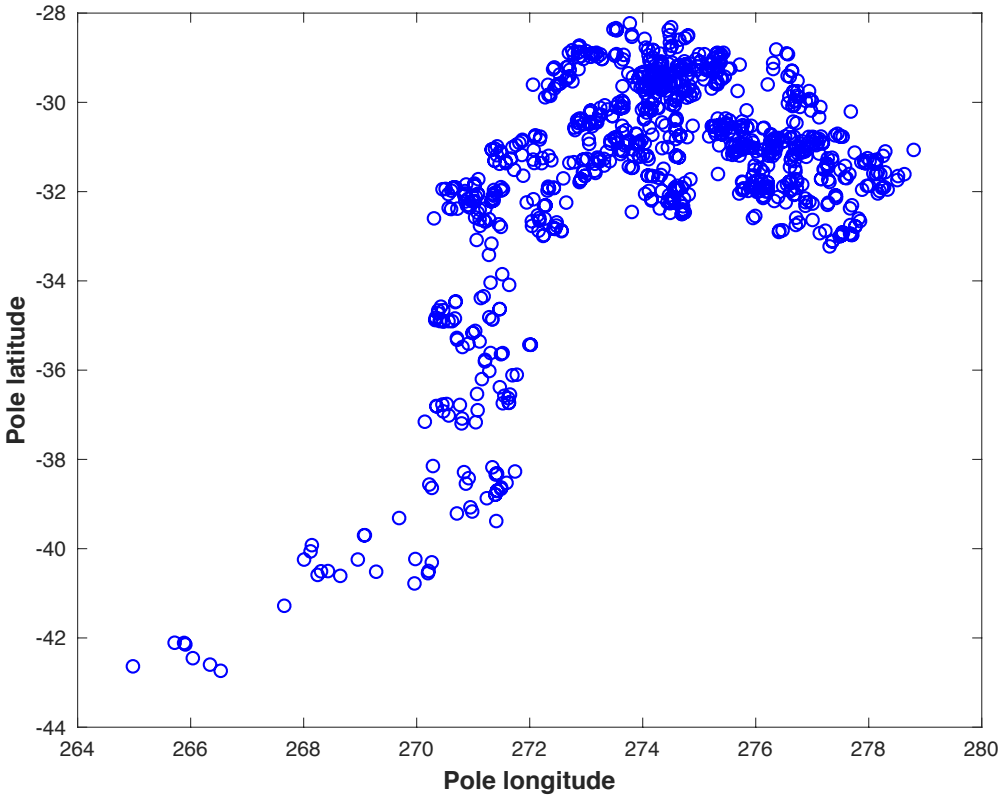

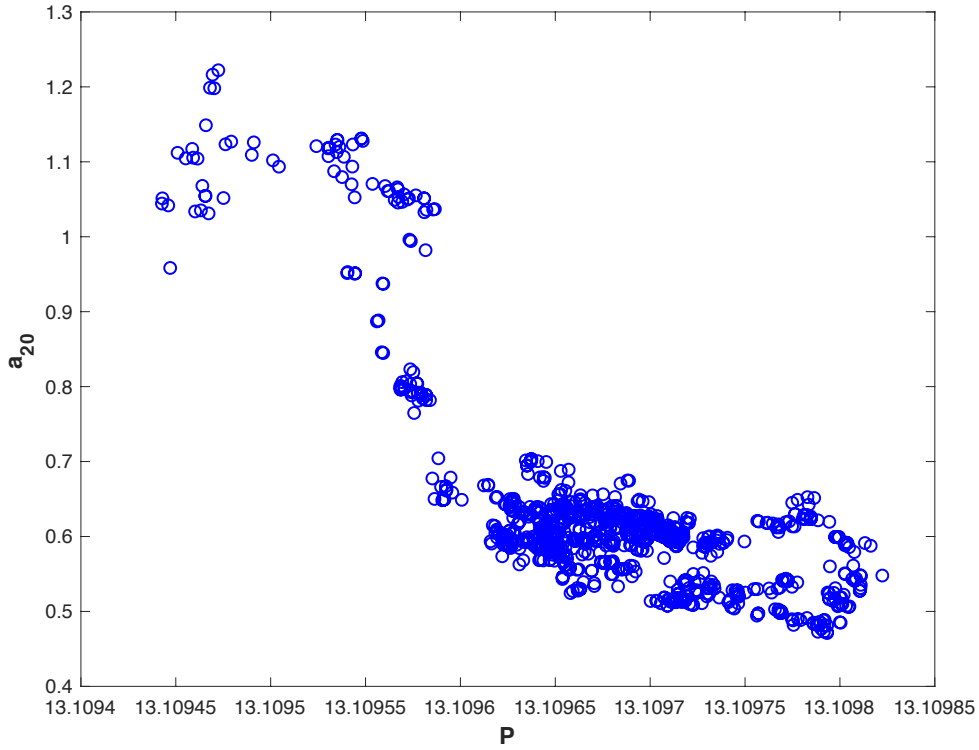
1.3
1.2
1.1
1
0.9
0.8
0.7
0.6
0.5
0.4
a20
13.1094
13.10945
13.1095
13.10955
13.1096
13.10965
13.1097
13.10975
13.1098
13.10985
P

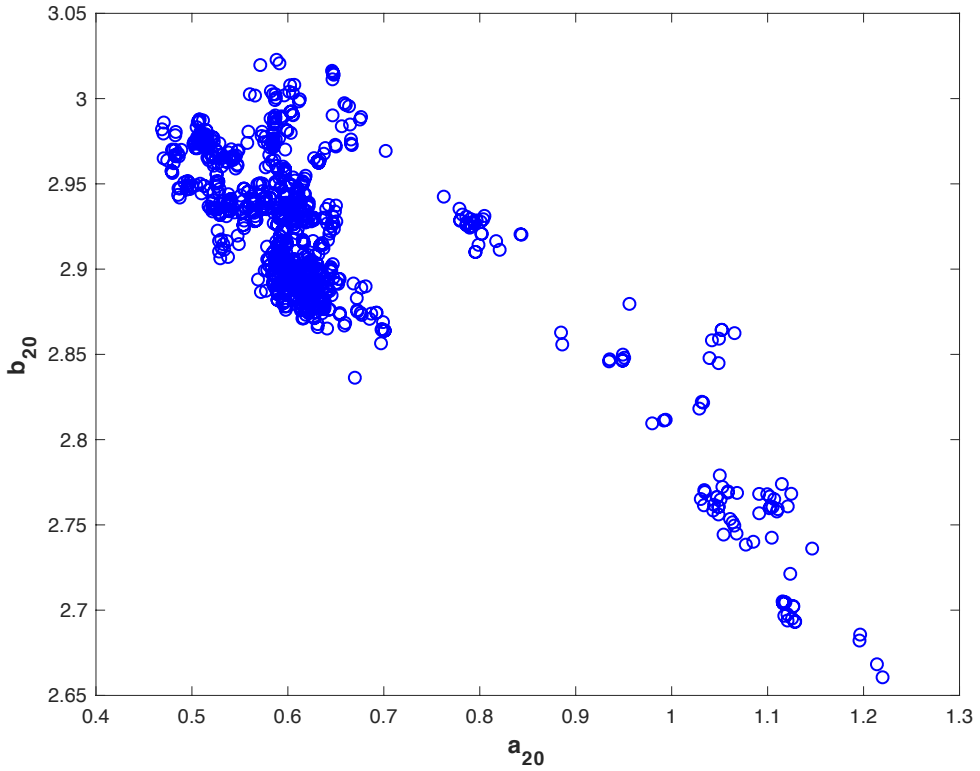
3.05
3
2.95
2.9
2.85
2.8
2.75
2.7
2.65
b20
0.4
0.5
0.6
0.7
0.8
0.9
1
1.1
1.2
1.3
a20

Convex inversion: (585) Bilkis

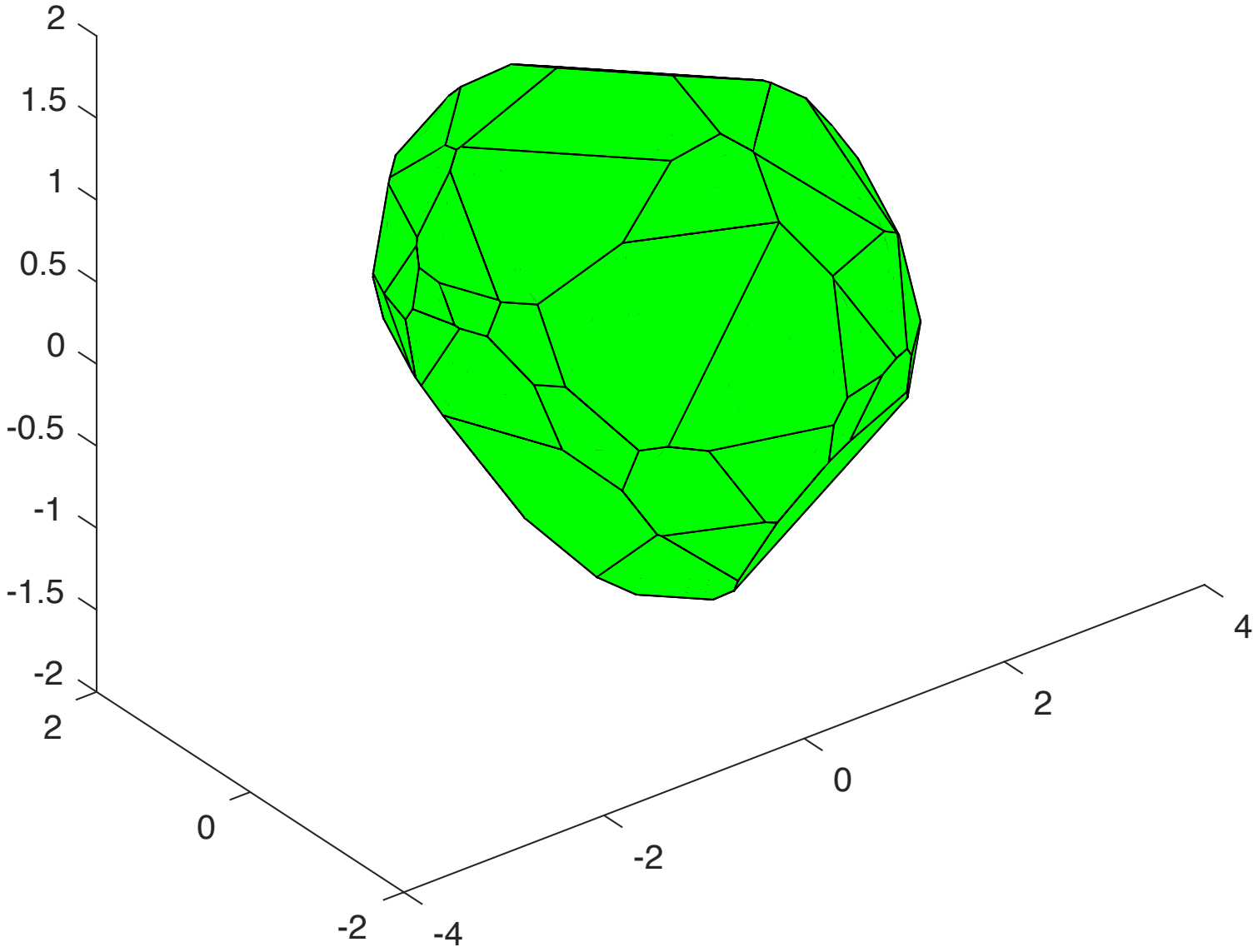

(585) Bilkis

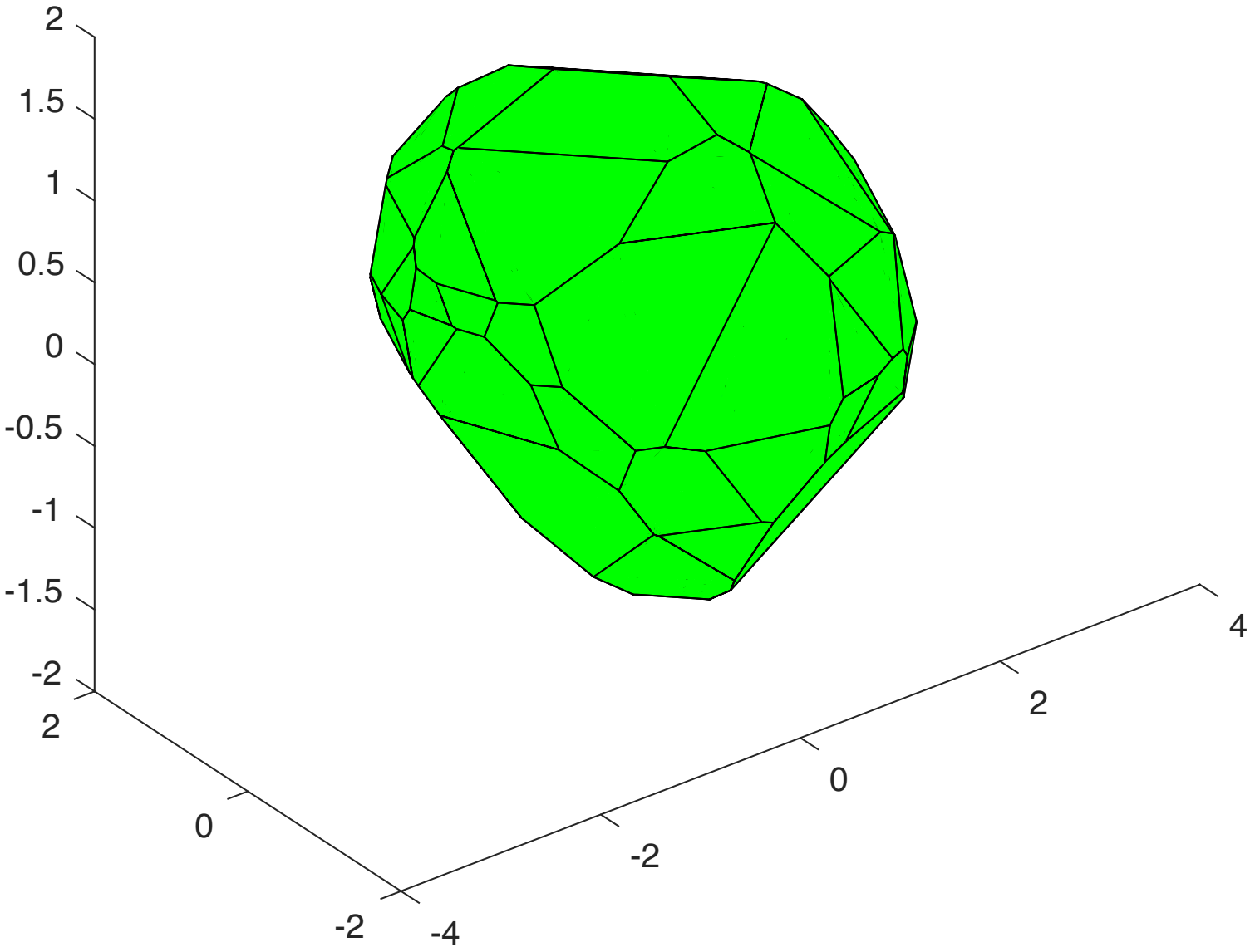

(21) Lutetia

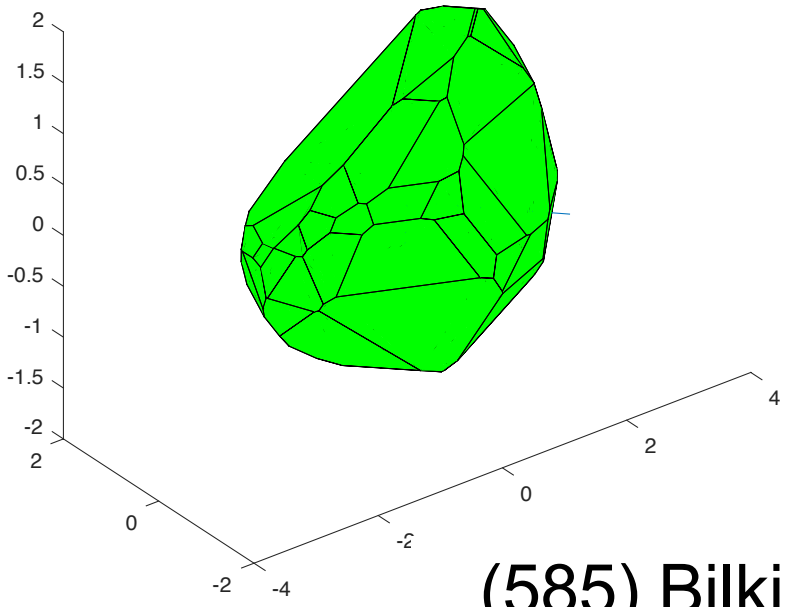

(26) Proserpina

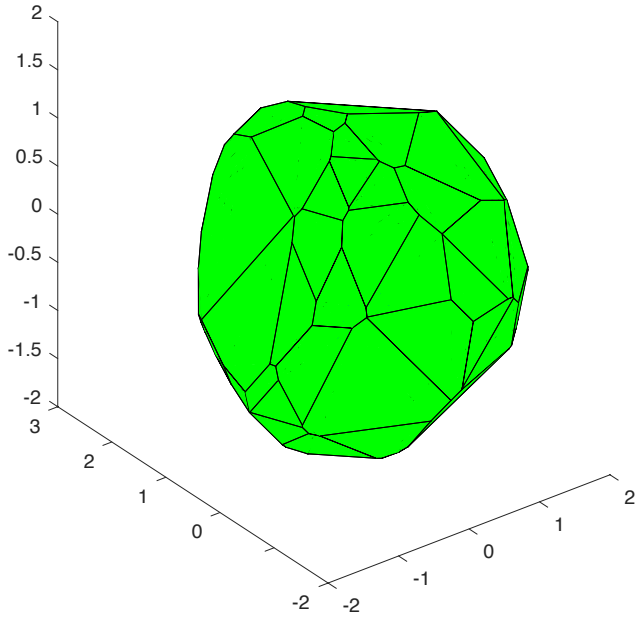

(585) Bilkis

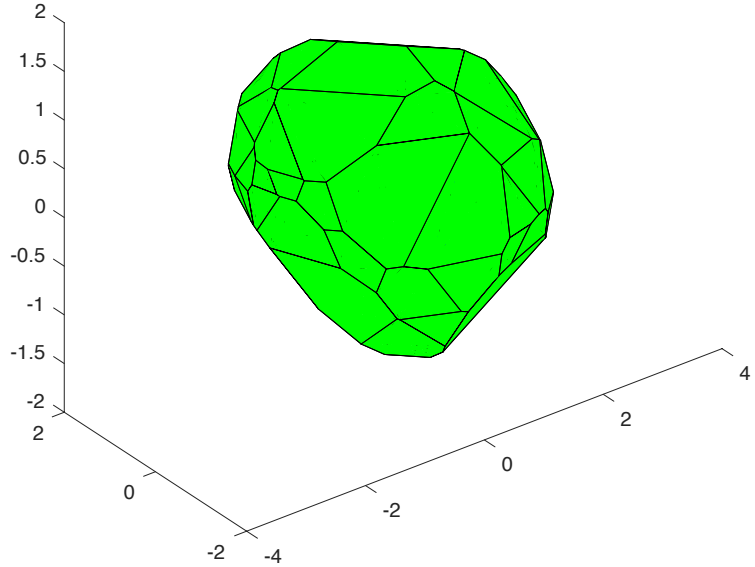

H, G_1, G_2 phase function

- Reduced magnitude expressed using three cubic-spline basis functions:

$$10^{-0.4V(\alpha)} = a_1 \Phi_1(\alpha) + a_2 \Phi_2(\alpha) + a_3 \Phi_3(\alpha)$$
$$= 10^{-0.4H}[G_1 \Phi_1(\alpha) + G_2 \Phi_2(\alpha) + (1 - G_1 - G_2)\Phi_3(\alpha)]$$

- Linear least-squares fitting for a_1, a_2, and a_3
- Muinonen et al., Icarus 209, 542, 2010

$$H = -2.5\log_{10}(a_1 + a_2 + a_3),$$
$$G_1 = \frac{a_1}{a_1 + a_2 + a_3},$$
$$G_2 = \frac{a_2}{a_1 + a_2 + a_3}.$$

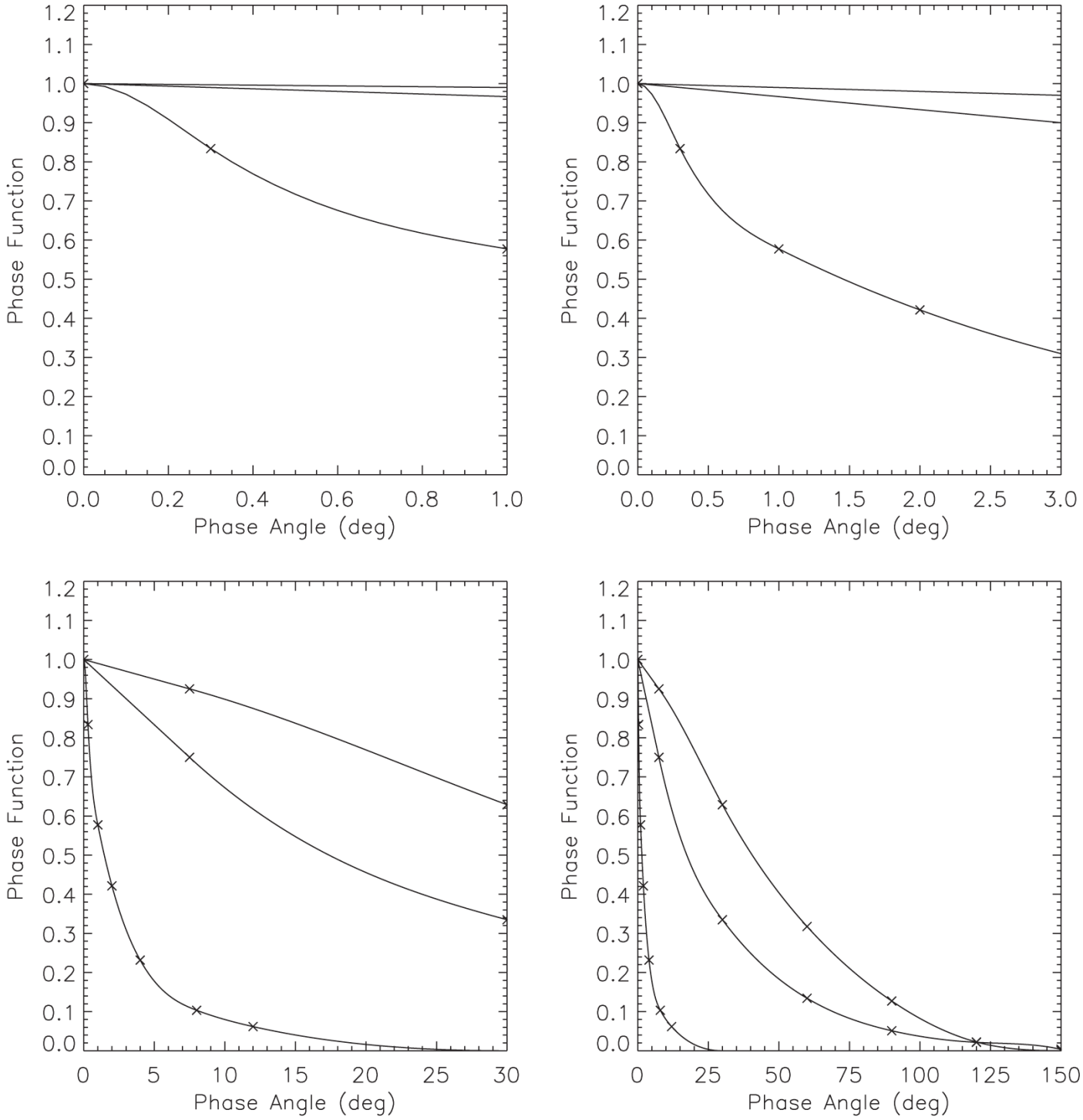
Phase Function
Phase Angle (deg)
0.0
0.1
0.2
0.3
0.4
0.5
0.6
0.7
0.8
0.9
1.0
1.1
1.2
0.0
0.2
0.4
0.6
0.8
1.0
0.0
0.5
1.0
1.5
2.0
2.5
3.0
0
5
10
15
20
25
30
0
25
50
75
100
125
150

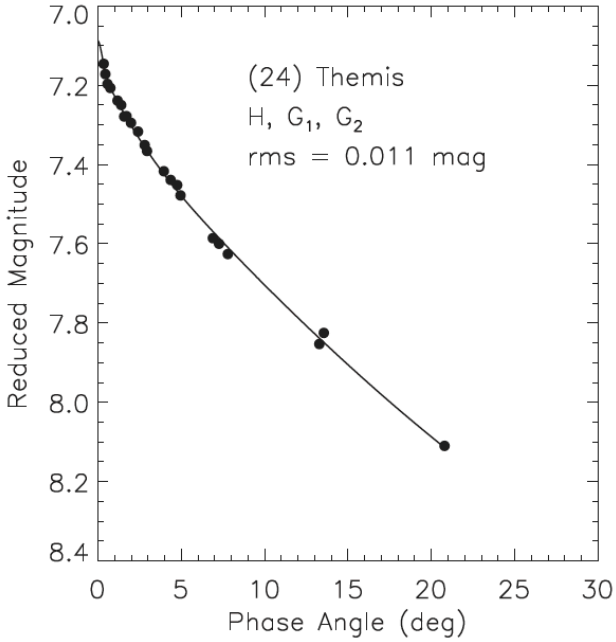
(24) Themis
H, G1, G2
rms = 0.011 mag
Reduced Magnitude
Phase Angle (deg)

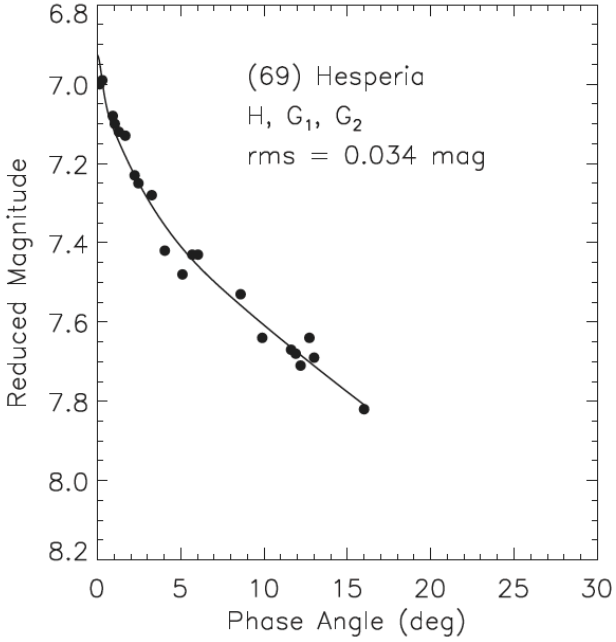
(69) Hesperia
H, G1, G2
rms = 0.034 mag
Reduced Magnitude
Phase Angle (deg)

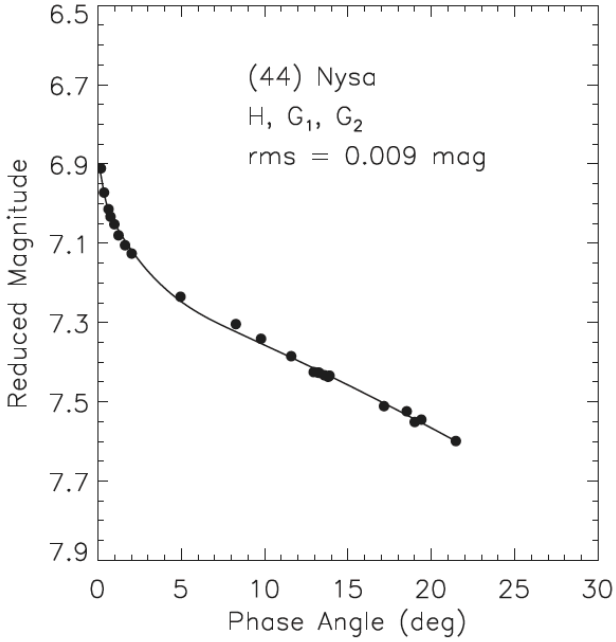
(44) Nysa
H, G1, G2
rms = 0.009 mag
Reduced Magnitude
Phase Angle (deg)

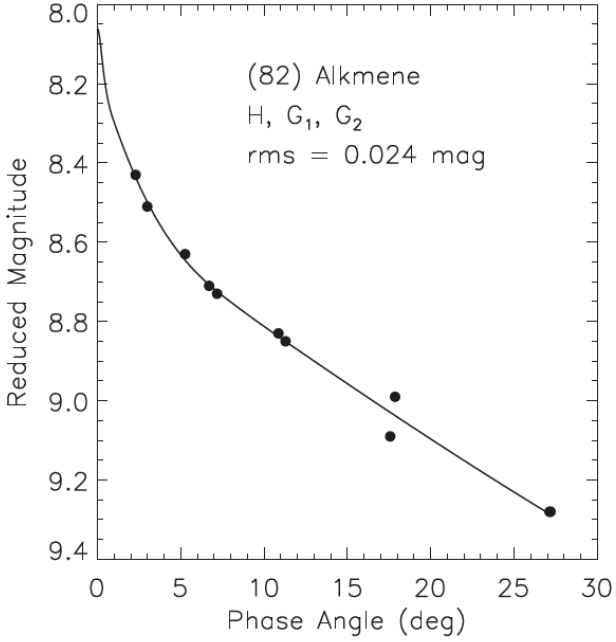
(82) Alkmene
H, G1, G2
rms = 0.024 mag
Reduced Magnitude
Phase Angle (deg)

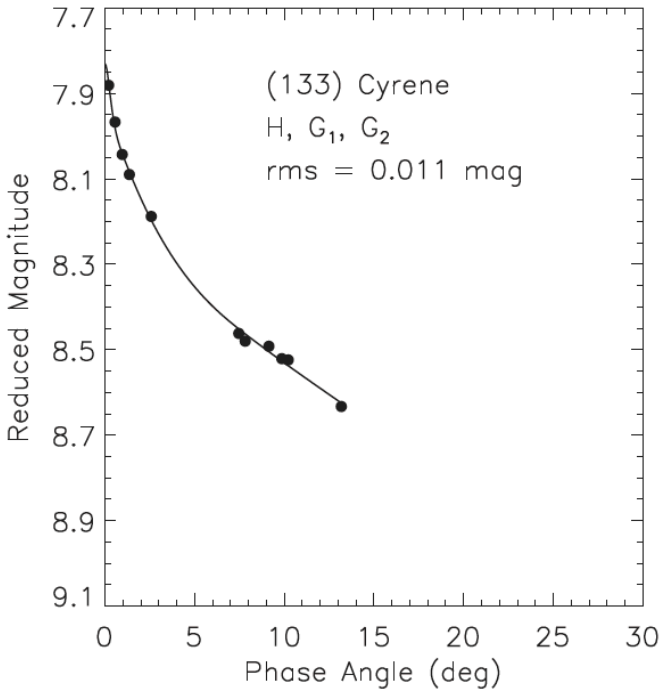
(133) Cyrene
H, G1, G2
rms = 0.011 mag
Reduced Magnitude
Phase Angle (deg)
7.7
7.9
8.1
8.3
8.5
8.7
8.9
9.1
0
5
10
15
20
25
30

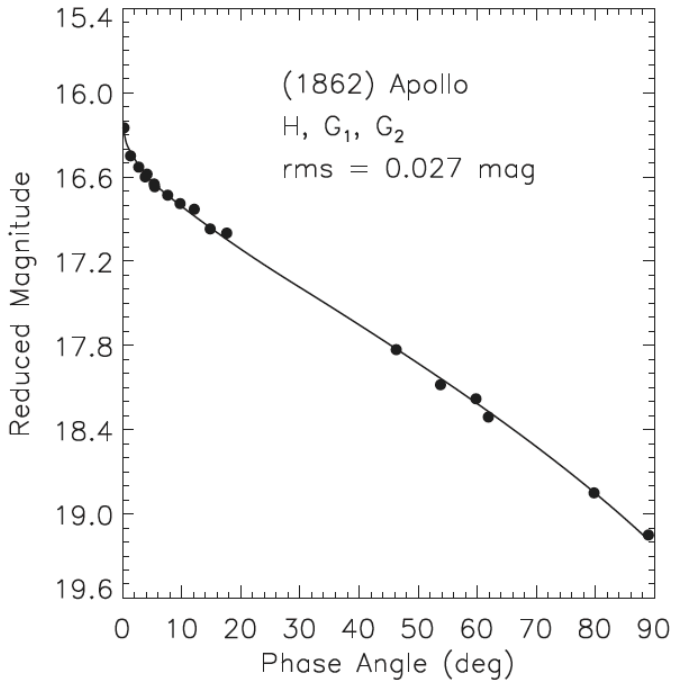
(1862) Apollo
H, G1, G2
rms = 0.027 mag
Reduced Magnitude
Phase Angle (deg)
15.4
16.0
16.6
17.2
17.8
18.4
19.0
19.6
0
10
20
30
40
50
60
70
80
90

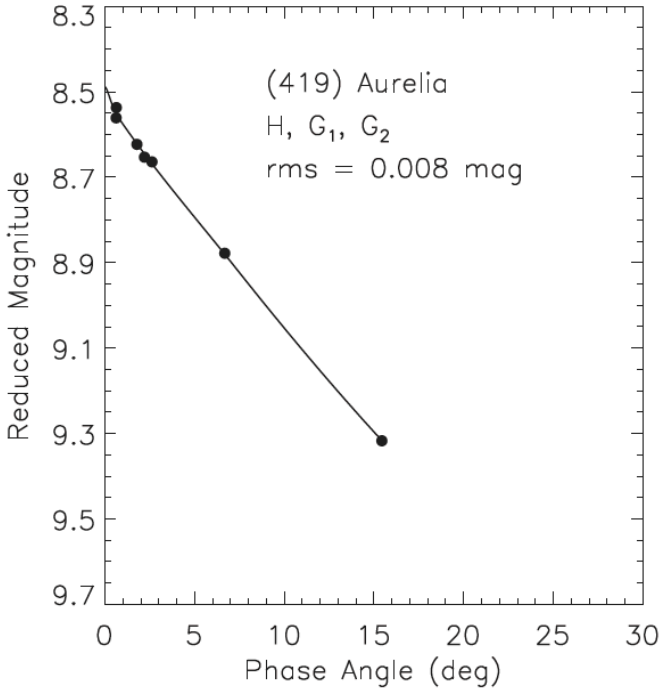
(419) Aurelia
H, G1, G2
rms = 0.008 mag
Reduced Magnitude
Phase Angle (deg)
8.3
8.5
8.7
8.9
9.1
9.3
9.5
9.7
0
5
10
15
20
25
30

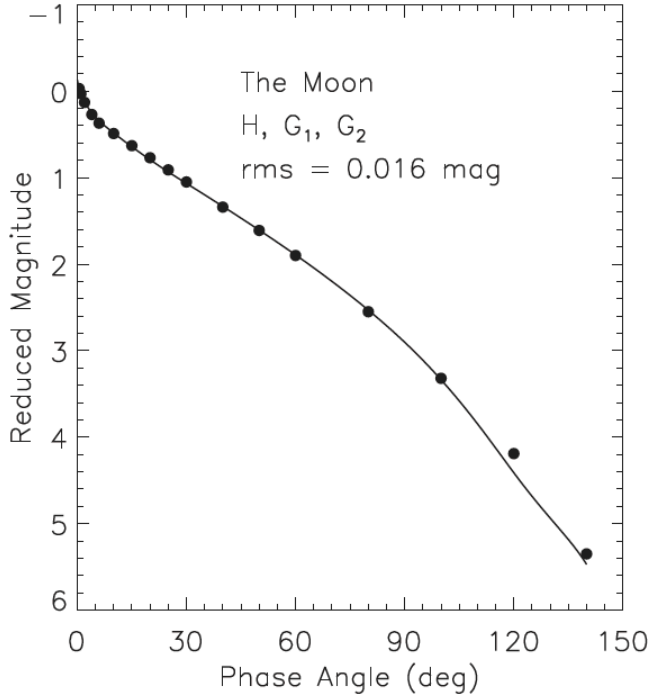
The Moon
H, G1, G2
rms = 0.016 mag
Reduced Magnitude
Phase Angle (deg)
−1
0
1
2
3
4
5
6
0
30
60
90
120
150

Table 1. The photometric G_1 and G_2 parameters for different asteroid classes in the single-parameter phase function by Penttilä et al. (2016).

Class	G_1	G_2
E	0.1505	0.6005
S/M	0.2588	0.3721
C	0.8228	0.0193
P	0.8343	0.0489
D	0.9617	0.0165

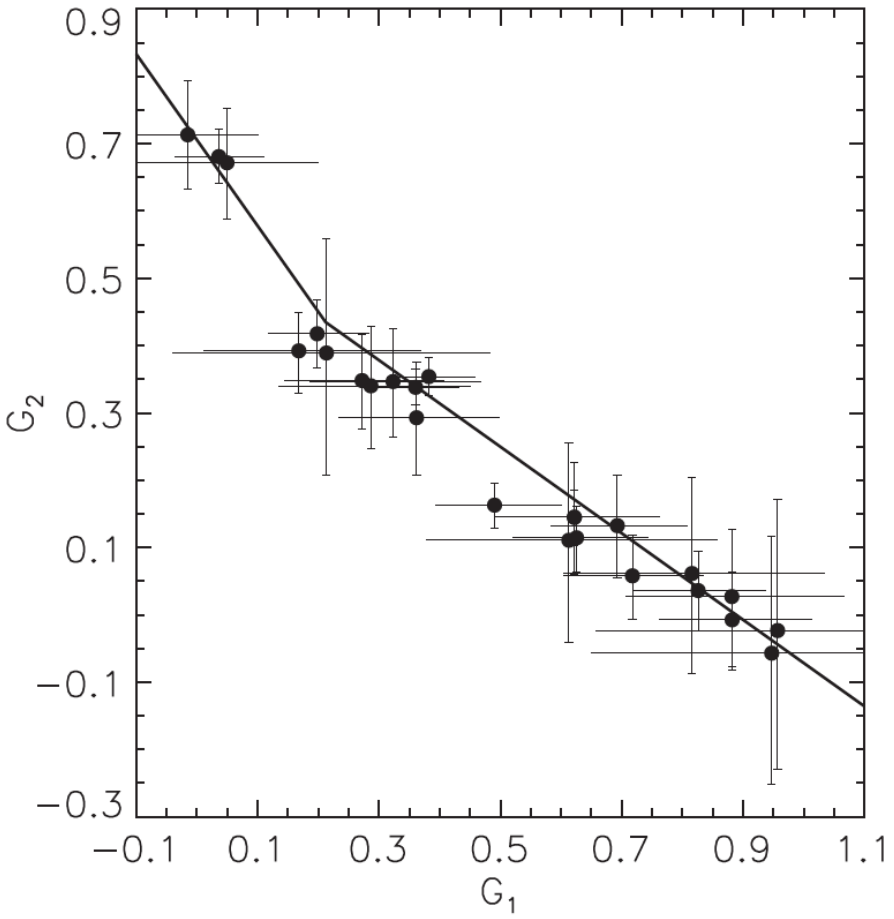

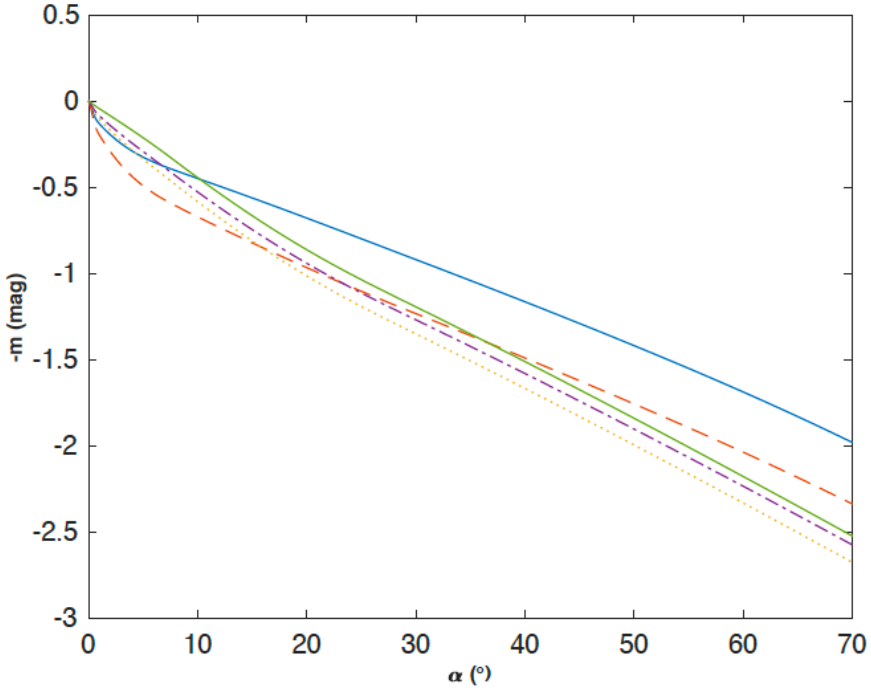

Fig. 1. The photometric phase curves pertaining to the five classes according to Penttilä et al. (2016): E (solid line, shallow), S/M (dashed line), C (dotted line), P (dash-dotted line), and D (solid line, steep). See Table 1.

Phase curves: (21) Lutetia

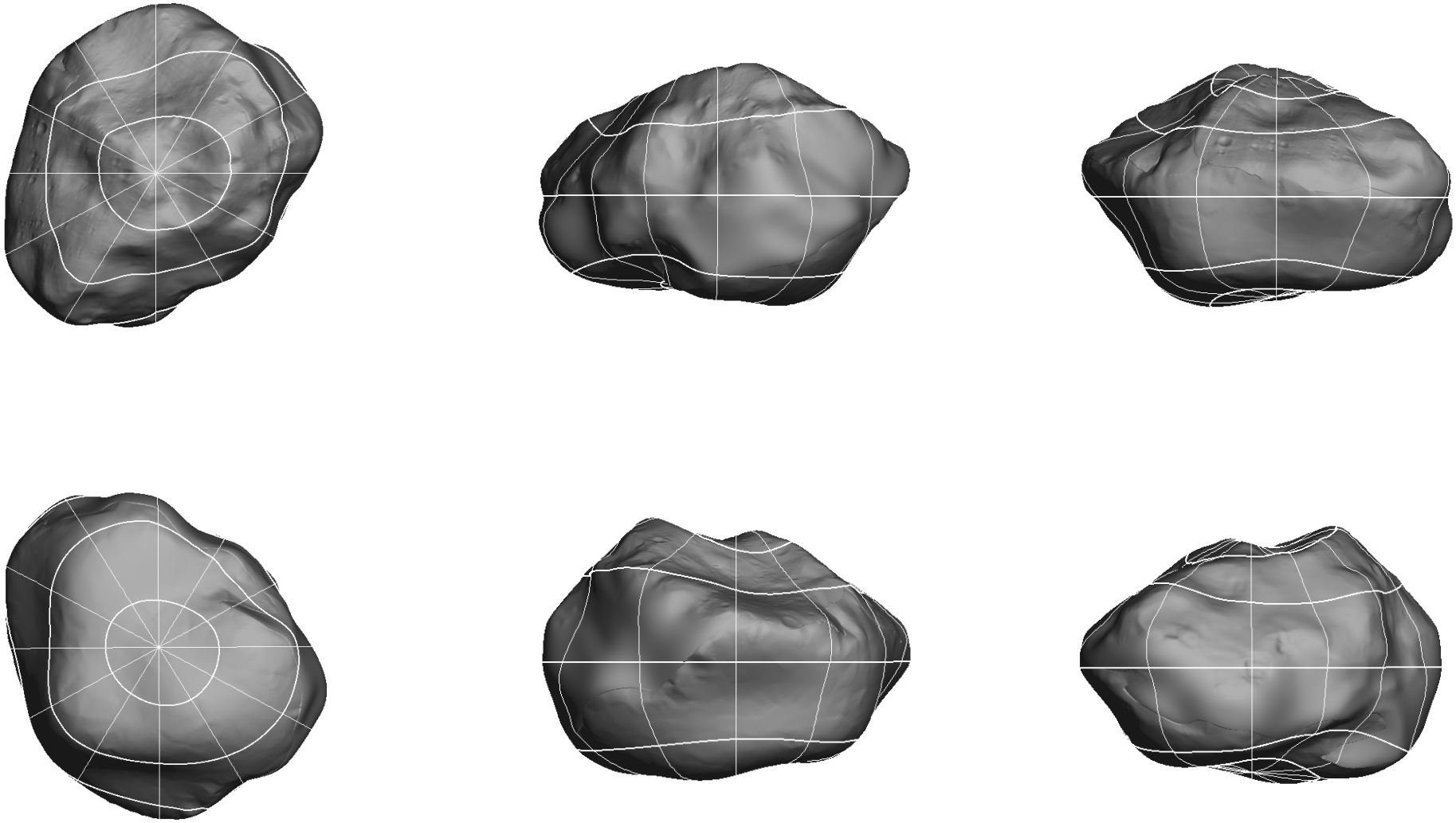

PDS

Gaia and groundbased data combined
(51 lightcurves, rms 0.03 mag)

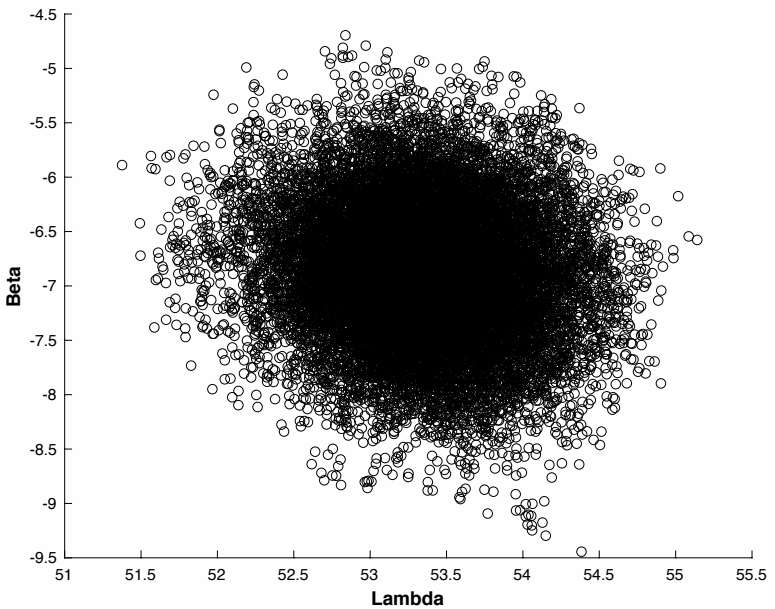

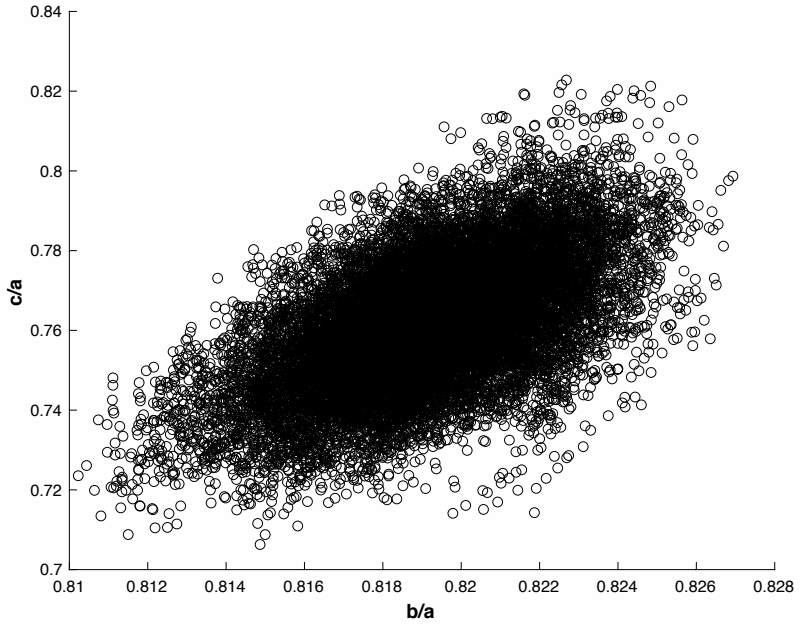

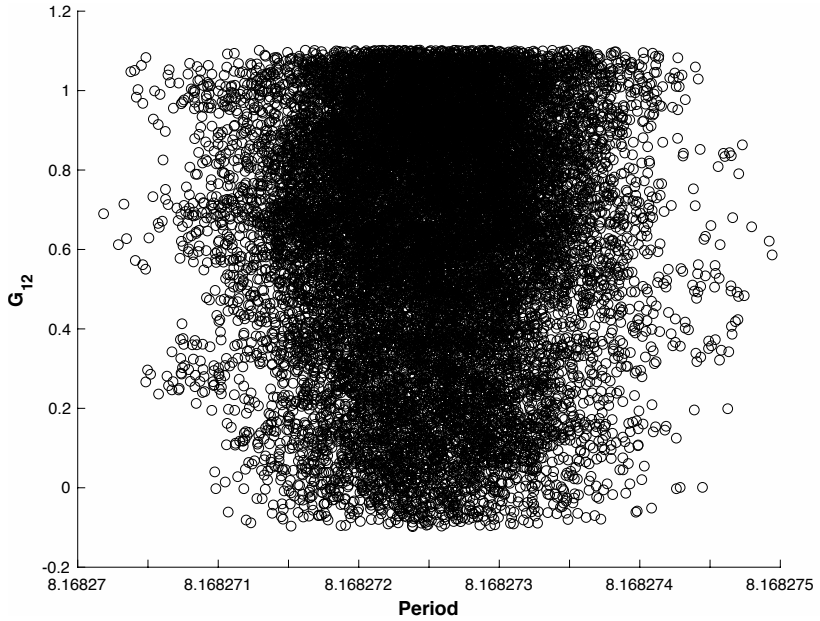

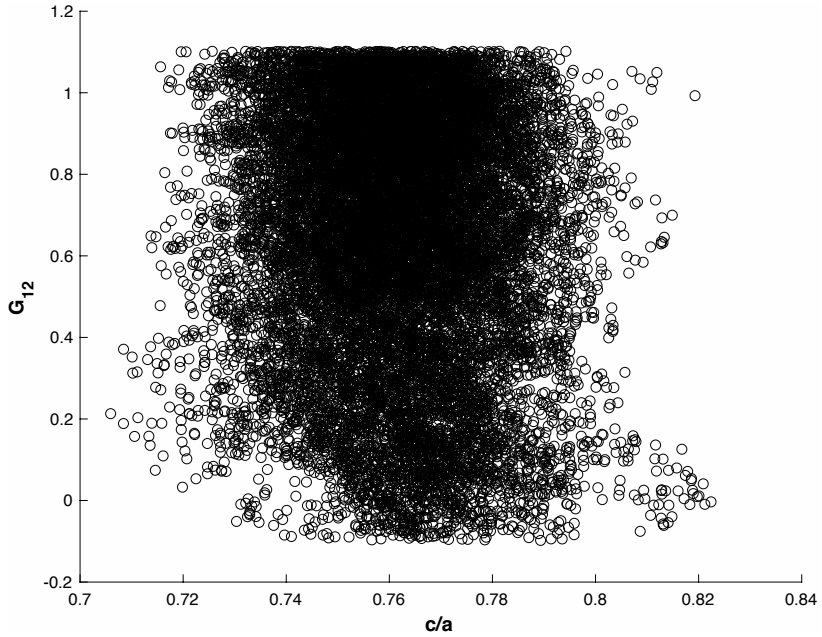

Phase curves: (2867) Steins

Muinonen et al. 2019

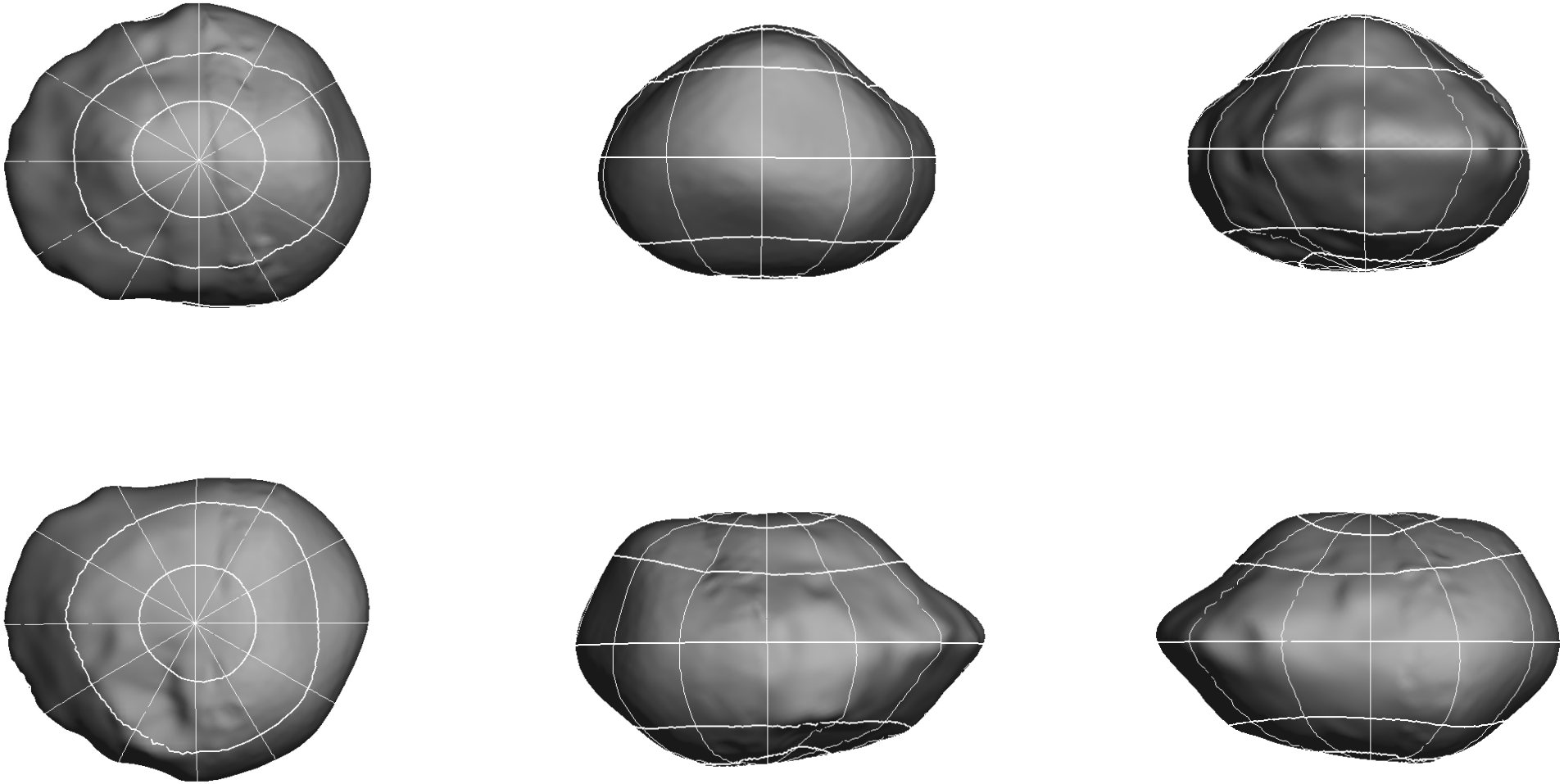

PDS

(2867) Steins

Karri Muinonen et al.

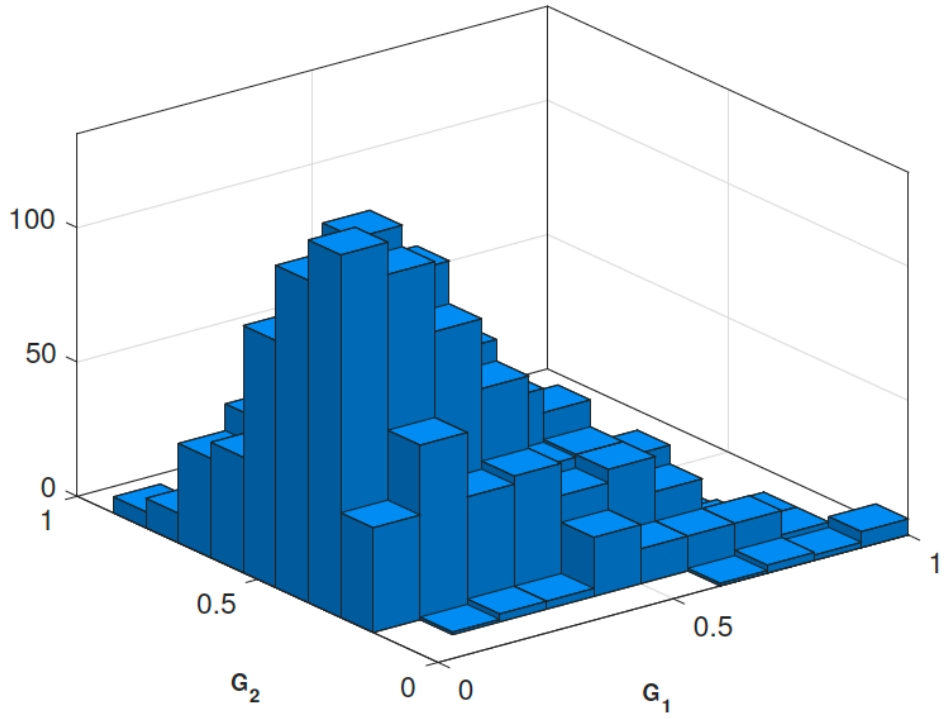

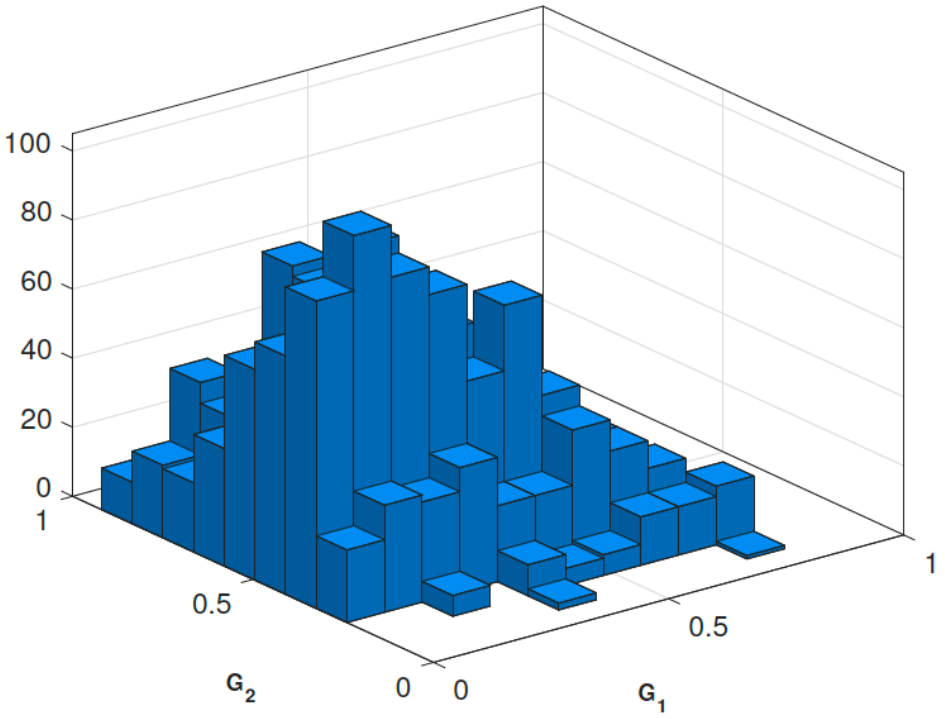

Photometric classification

11634 asteroids, from Gaia DR2

1898 asteroids, without priors

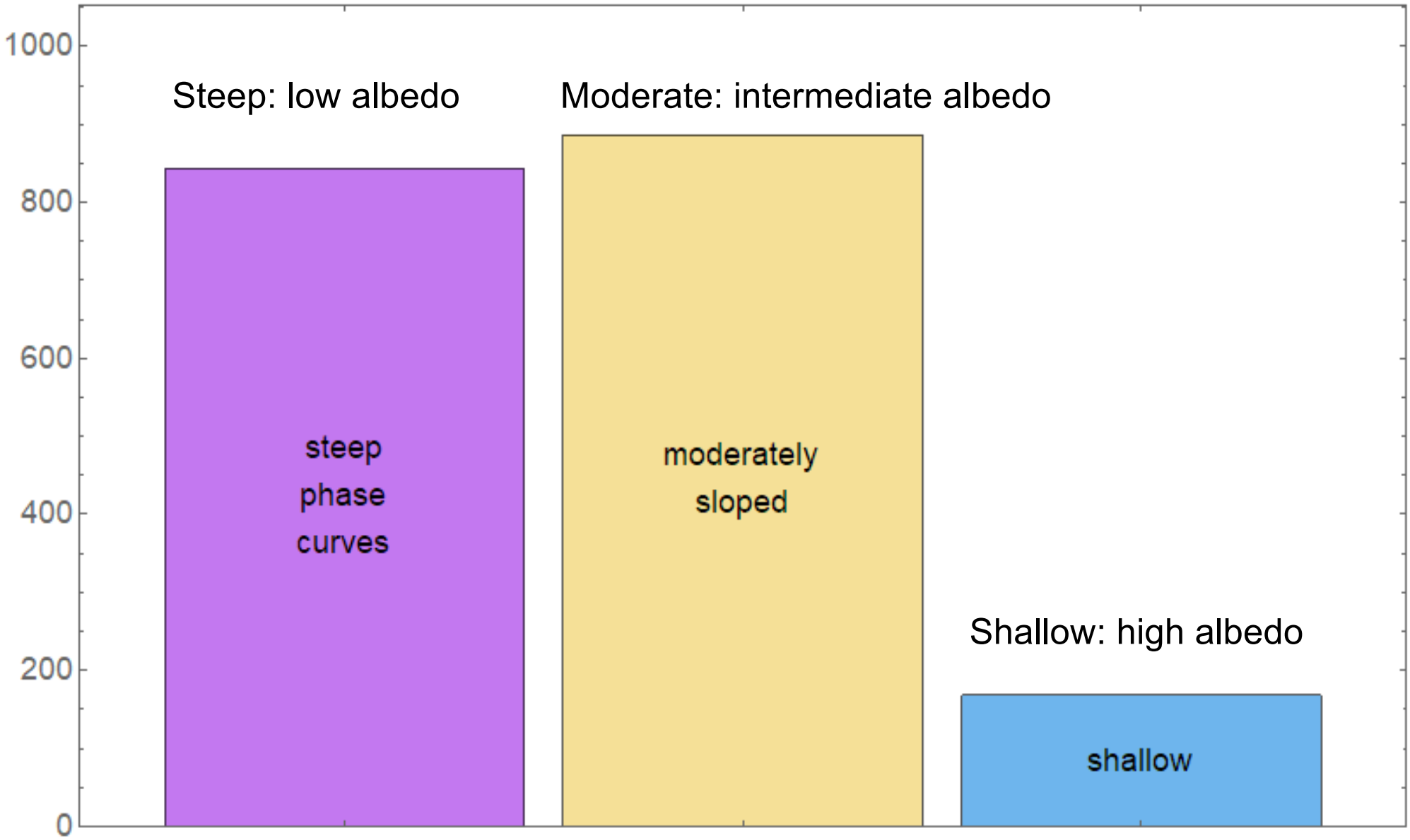

Preliminary results, Penttilä, Grön, Muinonen, et al., in prep.

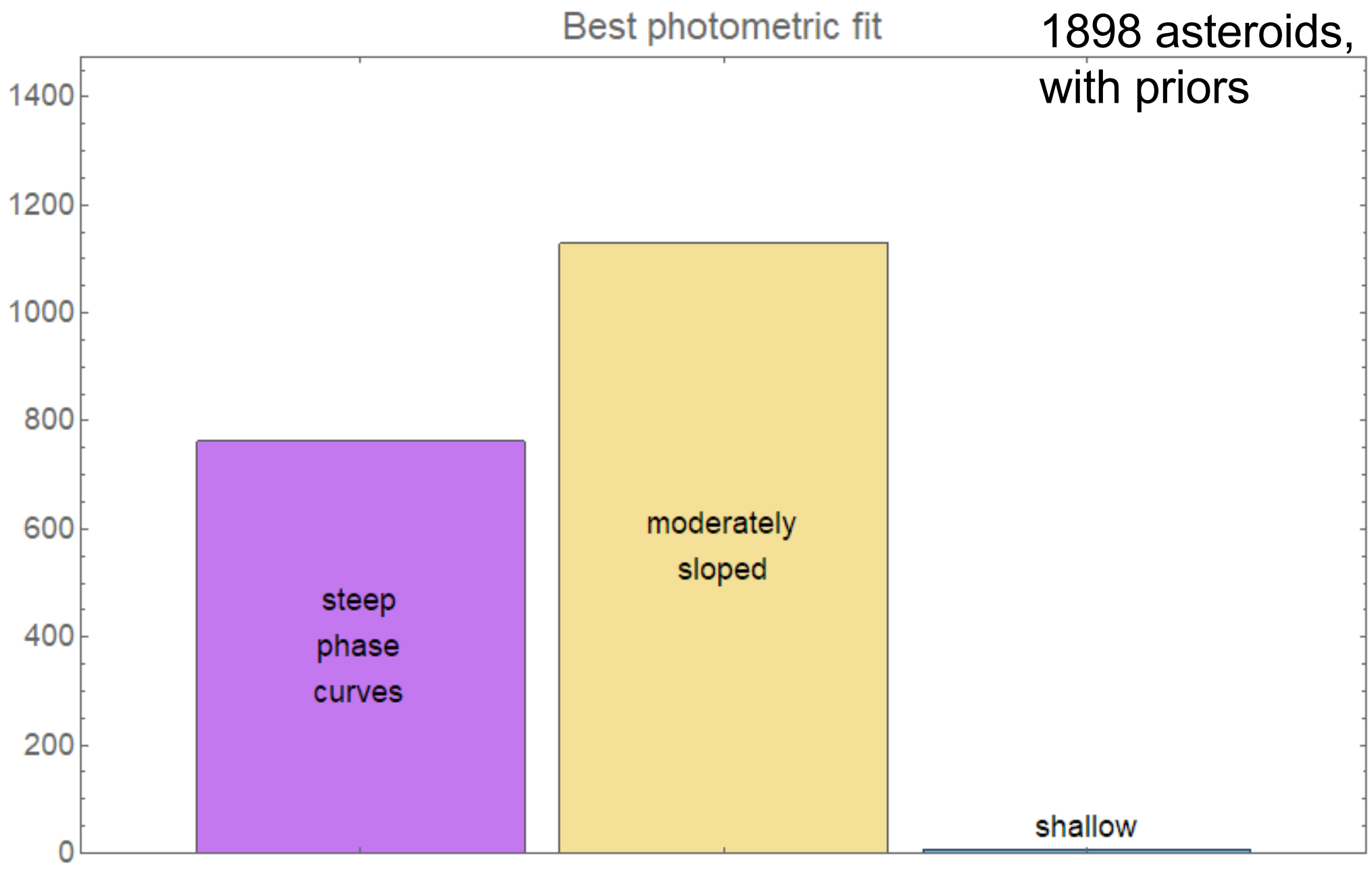
Best photometric fit
1898 asteroids,
with priors
1400
1200
1000
800
600
400
200
0
steep
phase
curves
moderately
sloped
shallow

Ellipsoid fit, case (a) 60.1 % correct in total		Classified to: steep phase curves	moderately sloped	shallow	total
Correct class from PDS Asteroid Taxonomy	steep phase curves	**63.0**	37.0	0.0	100 %
	moderately sloped	39.6	**60.4**	0.0	100 %
	shallow	0.0	100.0	**0.0**	100 %

173 asteroids with DAMIT rotations

Convex shape fit, case (b) 69.6 % correct in total		Classified to: steep phase curves	moderately sloped	shallow	total
Correct class from PDS Asteroid Taxonomy	steep phase curves	**73.0**	27.0	0.0	100 %
	moderately sloped	27.2	**69.3**	3.5	100 %
	shallow	0.0	100.0	**0.0**	100 %

173 asteroids with DAMIT rotations

Ellipsoid fit, case (c) 59.1 % correct in total		Classified to: steep phase curves	moderately sloped	shallow	total
Correct class from PDS Asteroid Taxonomy	steep phase curves	**57.1**	42.5	0.3	100 %
	moderately sloped	37.0	**62.7**	0.3	100 %
	shallow	50.0	50.0	**0.0**	100 %

626 asteroids with NASA PDS classifications

Laboratory experiments

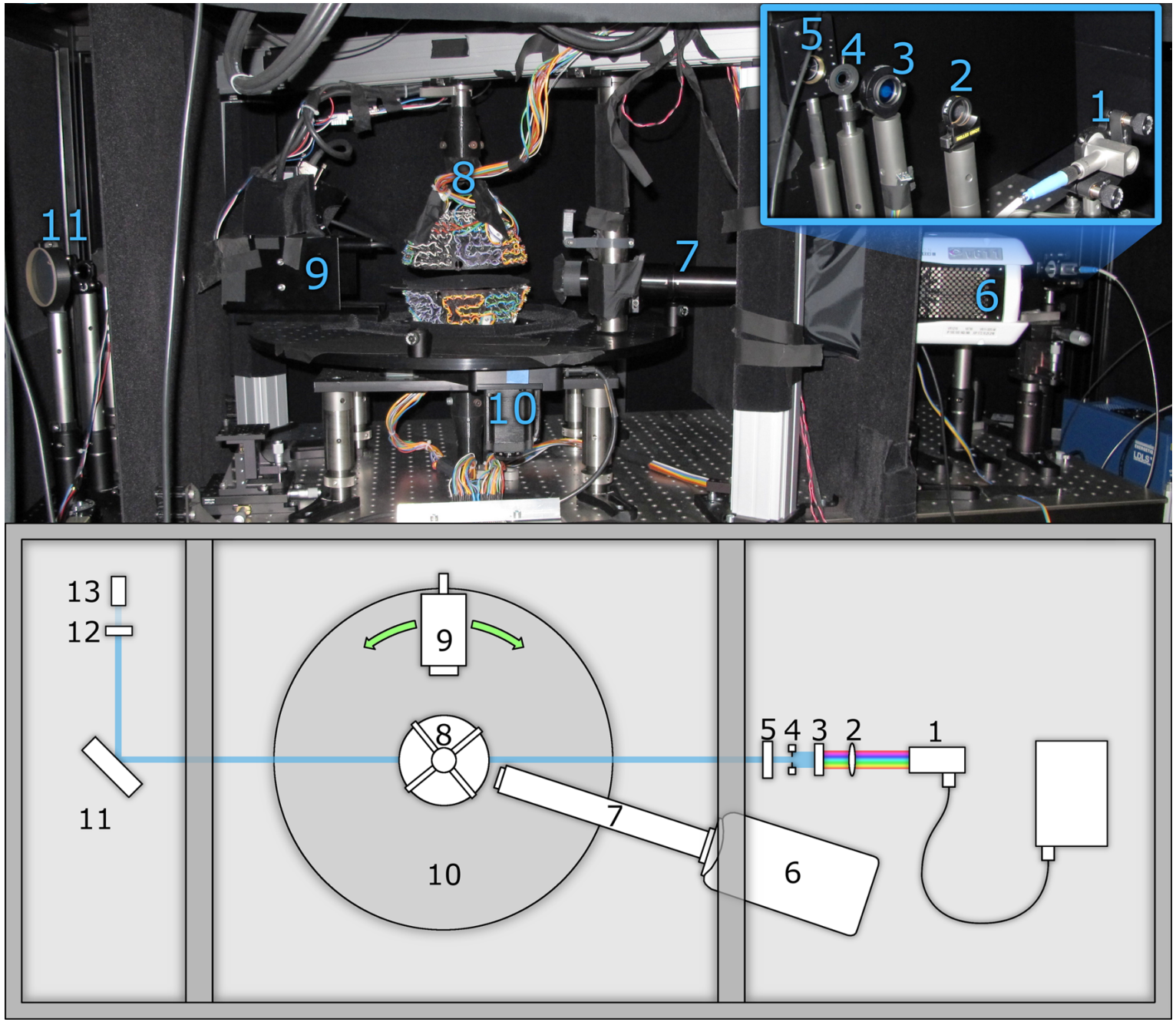

Maconi et al., JQSRT 2018


Orginal 100fps
3x speed
2mm

Conclusions

- Asteroid photometry from Gaia Data Release 2 validated
- Virtual-observation MCMC with ellipsoids and convex shapes validated
  - successful sampling in high-dimensional phase spaces ($N_{dim} > 80$)
- Proper phase curves have potential for photometric classification
  - reasonable with ellipsoids
  - promising with convex shapes
  - combine with spectroscopic classification
- Prospects for deriving proper geometric albedos and proper spherical albedos